

NASA CR-178,135

NASA Contractor Report 178135

ICASE REPORT NO. 84-66

NASA-CR-178135
19860021801

ICASE

METHODS FOR THE IDENTIFICATION OF MATERIAL PARAMETERS
IN DISTRIBUTED MODELS FOR FLEXIBLE STRUCTURES

H. T. Banks

J. M. Crowley

I. G. Rosen

Contract Nos. NAS1-16394, NAS1-17130

May 1986

FOR REFERENCE

NOT TO BE TAKEN FROM THIS ROOM

INSTITUTE FOR COMPUTER APPLICATIONS IN SCIENCE AND ENGINEERING
NASA Langley Research Center, Hampton, Virginia 23665

Operated by the Universities Space Research Association

NASA

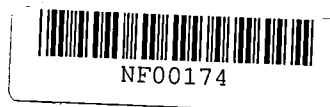
National Aeronautics and
Space Administration

Langley Research Center
Hampton, Virginia 23665

LIBRARY COPY

AUG 29 1986

LANGLEY RESEARCH CENTER
LIBRARY, NASA
HAMPTON, VIRGINIA



**METHODS FOR THE IDENTIFICATION OF MATERIAL PARAMETERS
IN DISTRIBUTED MODELS FOR FLEXIBLE STRUCTURES⁺**

H. T. Banks^{*}
Lefschetz Center for Dynamical Systems
Division of Applied Mathematics
Brown University
Providence, RI 02912

J. M. Crowley
Department of Mathematical Sciences
U. S. Air Force Academy
Academy, CO 80840

I. G. Rosen^{**}
Department of Mathematics
University of Southern California
Los Angeles, CA 90089

ABSTRACT

In this paper we present theoretical and numerical results for inverse problems involving estimation of spatially varying parameters such as stiffness and damping in distributed models for elastic structures such as Euler-Bernoulli beams. An outline of algorithms we have used and a summary of our computational experiences are presented.

^{*} This research was supported in part by the National Science Foundation under NSF Grant MCS-8504316, the Air Force Office of Scientific Research under Contract AFOSR-84-0398, and the National Aeronautics and Space Administration under NASA Grant NAG-1-517.

^{**} This research was supported in part by the Air Force Office of Scientific Research under Contract AFOSR-84-0393.

⁺ Part of this research was supported under NASA Contracts NAS1-16394 and NAS1-17130 while the authors were visiting scientists at the Institute for Computer Applications in Science and Engineering (ICASE), NASA Langley Research Center, Hampton, VA 23665-5225.

1. Introduction

In the past several years there has been an increased interest in the use of continuum models [13], [18], [22], [27], [28], [29], [30], in the study of large complex connected structures such as those being planned for deployment in space. These flexible platform and antenna structures, which are frequently composed of large lattice, panel and/or beam-like components, are typically constructed of graphite epoxy composite materials. Preliminary experimental testing suggests that one can expect significant material property changes (e.g., decreases in material damping by as much as 500%) due to ageing, environmental stress, fatigue, etc., during periods of deployment of structures composed of these composite materials. Therefore the identification or estimation of structural parameters (e.g., bending and shear rigidity, moments, damping, loading) will play an important role in the modeling, control and stabilization of these large space structures.

In recent efforts we (along with some of our colleagues and associates) have contributed to the research literature [2], [3], [4], [5], [8], [10], [11], [19], [25] in developing methodology (theoretical as well as computational) for such problems. In this paper we detail and extend some earlier results reported in [2], [4], [5] and [10]. Our specific aims here are twofold: (i) to present some of the ideas behind the theoretical results stated in [4] and [10], and (ii) to present a more extensive summary of some of our numerical findings for estimation of spatially dependent parameters, especially damping (again, earlier findings were presented in [4], [5] and [10]). To be more precise, we note that in many of the earlier efforts cited above, the focus was on convergence

results in a functional analytic framework (e.g., semigroups, dissipative operators, sesquilinear forms) and entailed certain smoothness (on the approximation elements) and compactness (on the admissible parameter sets) hypotheses. Here we present in §2 a theoretical approach (presented earlier in [4], [5] and treated in the context of hybrid systems describing the undamped vibration of beams with tip appendages in [10]) based on weak or variational arguments in the spirit of those from widely known "finite-elements" approaches to the approximation of partial differential equations (for a summary and numerous literature references, see [14]). This approach permits, in addition to relatively weak smoothness assumptions on approximation elements, a substantial relaxation of compactness assumptions on the admissible parameter sets. We comment further on this aspect of our presentation in §5 below and also refer the reader to [1] for a more complete discussion of weak vs. strong formulations in the context of inverse or parameter estimation problems.

In §3 we discuss implementation of some approximation ideas as we have employed them. Included is brief mention of the three principal optimization schemes we have used (sometimes in a hybrid method): a finite-difference Levenberg-Marquardt algorithm, a conjugate-gradient algorithm, and the popular Broyden-Fletcher-Goldfarb-Shanno algorithm. A summary of some of our numerical findings for a particular model (a damped Euler-Bernoulli beam) is given in §4 while the last section is devoted to a brief discussion of related and continuing efforts.

2. Theoretical Considerations

In this section we give a brief outline of convergence arguments associated with the algorithms and approximation ideas that we have used in obtaining the numerical results presented in subsequent sections. The arguments are applicable to quite general models of practical interest (e.g., see [10]) and we choose a specific simple model - a cantilevered Euler-Bernoulli beam with viscoelastic damping - only to illustrate the theoretical ideas.

We assume a normalized (mass = 1, length = 1) thin elastic beam with built-in or clamped end at $x = 0$, free end at $x = 1$, which is subject to Kelvin-Voigt damping. The equations for transverse vibrations embodied in the Euler-Bernoulli theory are given by (here $D = \partial/\partial x$)

$$(2.1) \quad u_{tt} + D^2\{q_1 D^2 u + q_2 D^2 u_t\} = f, \quad 0 < x < 1,$$

$$(2.2) \quad u(t, 0) = Du(t, 0) = 0, \quad t > 0,$$

$$(2.3) \quad \{q_1 D^2 u(t, \cdot) + q_2 D^2 u_t(t, \cdot)\} \Big|_{x=1} = 0,$$

$$(2.4) \quad [D\{q_1 D^2 u(t, \cdot) + q_2 D^2 u_t(t, \cdot)\}] \Big|_{x=1} = 0,$$

with initial data

$$(2.5) \quad u(0) = u_0$$

$$(2.6) \quad u_t(0) = v_0.$$

We assume here, for ease in exposition, that the initial data u_0 , v_0 are independent of the parameters $q = (q_1, q_2)$. The case $u_0 =$

$u_0(q), v_0 = v_0(q)$ can be treated with ideas similar to those given below. In the general case the loading term f may also depend on parameters to be estimated; again the arguments below are easily extended to cover such situations and we consider only the simple case $f = f(t, x)$.

The parameters q are restricted to lie in the admissible set

$$\tilde{Q} = \{q = (q_1, q_2) \mid q_i \in C[0, 1], \quad 0 < c_i \leq q_i(x) \leq v\}$$

where c_1, c_2, v are fixed constants. We remark that if no damping is present ($q_2 \equiv 0$), the convergence arguments outlined below can be made with even less effort.

We reformulate the system (2.1)-(2.6) in weak or variational form in the state spaces V and $H = L_2(0, 1)$ where

$$V = H_*^2 \equiv \{\psi \in H^2(0, 1) \mid \psi(0) = D\psi(0) = 0\}.$$

Denoting the usual inner product in $L_2(0, 1)$ by $\langle \cdot, \cdot \rangle$, we replace (2.1)-(2.4) by

$$(2.7) \quad \langle u_{tt}, \psi \rangle + \langle q_1 D^2 u + q_2 D^2 u_t, D^2 \psi \rangle = \langle f, \psi \rangle$$

and seek solutions u with $u(t) \in H_*^2$ satisfying (2.5) (2.6) and (2.7) for all $\psi \in H_*^2$.

Remark: As we have noted, other models can also be readily treated with the approach given here. For example, in the case of a simply supported beam, the boundary conditions (2.2)-(2.4) are replaced by $u(t, \eta) = D^2 u(t, \eta) = 0, \eta = 0, 1$ and the state space $V = H^2(0, 1) \cap H_0^1(0, 1)$ is used in place of H_*^2 .

When for example a tip mass of magnitude m is rigidly attached to the free end of the beam, the natural boundary condition (2.4) expressing zero shear is replaced by the ordinary differential equation

$$mu_{tt}(t,1) - [D\{q_1 D^2 u(t,\cdot) + q_2 D^2 u_t(t,\cdot)\}] \Big|_{x=1} = g(t)$$

where g is an external load applied to the tip mass in the transverse direction. In this case the appropriate choice for H is the product space $R \times L_2(0,1)$ with

$$V = \{(\eta, \psi) \in H: \psi \in H^2(0,1), \psi(0) = D\psi(0) = 0, \eta = \psi(1)\}$$

(see [10]). More will be said about our general approach in the context of hybrid systems (i.e. coupled systems of ordinary and partial differential equations) when we discuss specific examples and our numerical findings in Section 4.

It is not difficult to use standard arguments to show that (2.5), (2.6), (2.7) is well-posed. That is, under reasonable smoothness assumptions on f, u_0, v_0, q_1, q_2 and the positivity constraints of \tilde{Q} on q_1, q_2 , one can modify the arguments in [20, p. 272-281] to obtain existence of a unique solution u (on any finite interval $[0, T]$) satisfying $u \in C([0, T], V), u_t \in C([0, T], H), u_{tt} \in L_2([0, T], V')$ where $V = H_*^2(0,1), H = L_2(0,1)$ and V' is the dual of V with H as pivot space. Under additional smoothness hypotheses, one can

argue that this solution is actually a strong solution of (2.1)-(2.6) enjoying stronger smoothness properties (for example, see the results given in [10], [11]).

We consider a class of problems for the estimation of the parameters q_1, q_2 , given observations of the system (2.1)-(2.6). Given observations \tilde{u}_{ij} for $u(t_i, x_j)$ and a parameter set $Q \subset \tilde{Q}$, we seek $q^* \in Q$ to minimize over Q the least-squares criterion

$$(2.8) \quad J(q) = \sum_{i,j} |u(t_i, x_j; q) - \tilde{u}_{ij}|^2$$

where $u = u(q)$ is the solution to (2.5)-(2.7) corresponding to q .

Without additional assumptions on Q , these problems are intractable (from both a mathematical and computational viewpoint). We shall assume throughout that Q is compact in the $\mathcal{C}([0,1], \mathbb{R}^2)$ topology. Even with this compactness assumption, the minimization problem for (2.8) is infinite dimensional in both state and parameter space and thus is not readily solved without approximations.

For state space approximations $H^N \subset H_*^2$ we let H^N be finite dimensional, $N = 1, 2, \dots$, and let $P^N: L_2(0,1) \rightarrow H^N$ be the orthogonal projection of $L_2(0,1)$ onto H^N . We assume that H^N satisfies:

$$(2.9) \quad \text{For each } \psi \in L_2(0,T; H_*^2), P^N \psi \rightarrow \psi \text{ in } L_2(0,T; H_*^2).$$

These hypotheses are satisfied by a number of useful and popular families of approximations: quintic or cubic B-splines modified to satisfy the boundary conditions defining H_*^2 (see [2], [26]); Hermite cubic splines (modified); etc.

For parameter set approximations Q^M , we suppose that Q^M is given by $Q^M = i_M(Q)$ where the set Q^M and the mapping $i_M : Q \rightarrow C([0,1], R^2)$ satisfy:

$$(2.10) \quad Q^M \text{ is compact in the } \mathcal{L} \text{ topology;}$$

$$(2.11) \quad i_M(q) \rightarrow q \text{ in the } \mathcal{L} \text{ topology, uniformly in } q \in Q.$$

These conditions are relatively mild and include some practically useful approximation schemes such as linear and cubic interpolatory splines (for discussions, see [7], [9]). We note that we do not require $Q^M \subset \tilde{Q}$, although in some situations this may be automatically satisfied. In other cases it may be desirable to impose the constraints in \tilde{Q} explicitly in using the sets Q^M in computational examples.

For any $q \in \tilde{Q}$, we may define in H^N approximating systems for (2.5)-(2.7) as follows: we seek $u^N(t) \in H^N$ such that for all $\psi \in H^N$

$$(2.12) \quad \langle u_{tt}^N, \psi \rangle + \langle q_1 D^2 u^N + q_2 D^2 u_t^N, D^2 \psi \rangle = \langle f, \psi \rangle$$

$$(2.13) \quad u^N(0) = P^N u_0$$

$$(2.14) \quad u_t^N(0) = P^N v_0.$$

We then define, for approximation indices (N, M) , the approximating estimation problems:

Minimize

$$(2.15) \quad J^N(q) = \sum_{i,j} |u^N(t_i, x_j; q) - \tilde{u}_{ij}|^2$$

over $q \in Q^M$, where u^N is the solution of (2.12)-(2.14).

Let \hat{q}_M^N be solutions of the (N, M) estimation problems, $N = 1, 2, \dots$, $M = 1, 2, \dots$ (Such solutions exist since Q^M is compact in \mathcal{L} and $q \rightarrow J^N(q)$ is continuous in the \mathcal{L} topology.) Since $\hat{q}_M^N \in Q^M = i_M(Q)$, there exist \bar{q}_M^N in Q such that $i_M(\bar{q}_M^N) = \hat{q}_M^N$. The \mathcal{L} compactness of Q implies the existence of a convergent subsequence $\{\bar{q}_{M_k}^{N_j}\}$ of $\{\bar{q}_M^N\}$ with $\bar{q}_{M_k}^{N_j} \rightarrow \hat{q} \in Q$ as $N_j \rightarrow \infty$, $M_k \rightarrow \infty$.

The limit function \hat{q} is an obvious candidate for a solution to the problem for (2.8). To see that it does indeed provide a minimum for (2.8), we first observe that property (2.11) for i_M along with the inequality

$$\left| \hat{q}_{M_k}^{N_j} - \hat{q} \right| \leq \left| i_{M_k}(\bar{q}_{M_k}^{N_j}) - \bar{q}_{M_k}^{N_j} \right| + \left| \bar{q}_{M_k}^{N_j} - \hat{q} \right|$$

guarantees that $\{\hat{q}_{M_k}^{N_j}\}$ also converges to \hat{q} in \mathcal{L} . Next we have by definition

$$J^{N_j}(\hat{q}_{M_k}^{N_j}) \leq J^{N_j}(\tilde{q}) \quad \text{for all } \tilde{q} \in Q^{M_k}$$

or

$$J^{N_j}(\hat{q}_{M_k}^{N_j}) \leq J^{N_j}(i_{M_k}(q)) \quad \text{for all } q \in Q.$$

Thus, taking the limit as $N_j \rightarrow \infty$, $M_k \rightarrow \infty$ yields the desired inequality

$$J(\hat{q}) \leq J(q) \quad \text{for all } q \in Q,$$

if we can argue $J^N(q^n) \rightarrow J(q)$ as $N \rightarrow \infty, n \rightarrow \infty$, for any sequence $\{q^n\}$ with $q^n \rightarrow q$ in \mathcal{Q} . But this follows immediately once we have argued that $u^N(t_i, x_j; q^n) \rightarrow u(t_i, x_j; q)$ for arbitrary $q^n \rightarrow q$. The remainder of this section will be devoted to a sketch of arguments for this convergence.

We recall (2.5)-(2.7) and (2.12)-(2.14) where we must consider $u^N(q^n), u(q)$ with $N \rightarrow \infty, n \rightarrow \infty, q^n \rightarrow q$. Simple reindexing arguments reveal that it suffices to argue that $u^N(q^N) \rightarrow u(q)$ as $N \rightarrow \infty$ for arbitrary sequences $\{q^N\}$ with $q^N \rightarrow q$ as $N \rightarrow \infty$. Here, of course, $u^N(q)$ and $u(q)$ are the solutions of (2.12)-(2.14) and (2.5)-(2.7), respectively, corresponding to q .

Let $q^N \rightarrow q$ be arbitrary and let u^N, u denote $u^N(q^N), u(q)$ throughout below. We define

$$z^N = u^N(q^N) - P^N u(q).$$

Then (2.5), (2.6), (2.13), (2.14) imply that $z^N(0) = z_t^N(0) = 0$ (in cases where u_0, v_0 depend on q , the arguments differ slightly since then $z^N(0), z_t^N(0)$ are not zero, but approach zero as $N \rightarrow \infty$ under suitable smoothness assumptions on u_0, v_0). Using (2.7) and (2.12) we have for $\psi \in H^N \subset H_\star^2$

$$\begin{aligned}
 \langle z_{tt}^N, \psi \rangle &= \langle u_{tt}^N - u_{tt} + u_{tt} - P^N u_{tt}, \psi \rangle \\
 (2.16) \quad &= \langle q_1 D^2 u - q_1^N D^2 u^N, D^2 \psi \rangle + \langle q_2 D^2 u_t - q_2^N D^2 u_t^N, D^2 \psi \rangle \\
 &+ \langle (I - P^N) u_{tt}, \psi \rangle .
 \end{aligned}$$

(If f depends on unknown parameters q we would also have a term $\langle f(q^N) - f(q), \psi \rangle$ above but the essential features of our presentation would again remain the same.)

Adding appropriate terms to both sides of (2.16), we find

$$\begin{aligned}
 \langle z_{tt}^N, \psi \rangle &+ \langle q_1^N D^2 z^N, D^2 \psi \rangle + \langle q_2^N D^2 z_t^N, D^2 \psi \rangle \\
 (2.17) \quad &= \langle q_1 D^2 u - q_1^N D^2 P^N u, D^2 \psi \rangle + \langle q_2 D^2 u_t - q_2^N D^2 P^N u_t, D^2 \psi \rangle \\
 &+ \langle (I - P^N) u_{tt}, \psi \rangle .
 \end{aligned}$$

Choosing $\psi = z_t^N$ (which is in H^N), we obtain

$$\begin{aligned}
 &\frac{1}{2} \frac{d}{dt} \left\{ \left| z_t^N \right|^2 + \left| \sqrt{q_1^N} D^2 z^N \right|^2 \right\} + \left| \sqrt{q_2^N} D^2 z_t^N \right|^2 \\
 &= \langle \Delta_1^N, D^2 z_t^N \rangle + \langle \Delta_{2t}^N, D^2 z_t^N \rangle + \langle \delta^N, z_t^N \rangle
 \end{aligned}$$

where $\Delta_i^N \equiv q_i D^2 u - q_i^N D^2 P^N u$ and $\delta^N \equiv (I - P^N) u_{tt}$.

This implies (since $q_2(x) \geq c_2$)

$$\begin{aligned}
 &\frac{1}{2} \frac{d}{dt} \left\{ \left| z_t^N \right|^2 + \left| \sqrt{q_1^N} D^2 z^N \right|^2 \right\} + c_2 \left| D^2 z_t^N \right|^2 \\
 &\leq \frac{d}{dt} \langle \Delta_1^N, D^2 z^N \rangle - \langle \Delta_{1t}^N, D^2 z^N \rangle \\
 &+ \frac{1}{4c_2} \left| \Delta_{2t}^N \right|^2 + c_2 \left| D^2 z_t^N \right|^2 + \langle \delta^N, z_t^N \rangle .
 \end{aligned}$$

(If damping is present, but we are only guaranteed $q_2(x) \geq 0$, the arguments must be modified at this step, but again the essential ideas are similar to our presentation here.) From this last inequality we have

$$\begin{aligned} \frac{d}{dt} \left\{ \left| z_t^N \right|^2 + \left| \sqrt{q_1^N} D^2 z^N \right|^2 - 2 \langle \Delta_1^N, D^2 z^N \rangle \right\} \\ \leq 2 \left| \langle \Delta_{1t}^N, D^2 z^N \rangle \right| + \frac{1}{2c_2} \left| \Delta_{2t}^N \right|^2 + 2 \langle \delta^N, z_t^N \rangle. \end{aligned}$$

Integration of this inequality leads to

$$\begin{aligned} \left| z_t^N \right|^2 + \left| \sqrt{q_1^N} D^2 z^N \right|^2 \leq \left| z_t^N(0) \right|^2 + \left| \sqrt{q_1^N} D^2 z^N(0) \right|^2 + 2 \langle \Delta_1^N, D^2 z^N \rangle \\ - \langle \Delta_1^N(0), D^2 z^N(0) \rangle \\ + \int_0^t \left\{ 2 \left| \langle \Delta_{1t}^N, D^2 z^N \rangle \right| + \frac{1}{2c_2} \left| \Delta_{2t}^N \right|^2 + 2 \langle \delta^N, z_t^N \rangle \right\} ds. \end{aligned}$$

In the case we are considering here (u_0, v_0 independent of q), we have $z_t^N(0) = 0$ and one also can easily argue that $D^2 z^N(0) = 0$. We therefore find

$$\begin{aligned} \left| z_t^N \right|^2 + c_1 \left| D^2 z^N \right|^2 \leq \frac{2}{c_1} \left| \Delta_1^N \right|^2 + \frac{c_1}{2} \left| D^2 z^N \right|^2 \\ + \int_0^T \left\{ \frac{1}{2c_2} \left| \Delta_{2t}^N \right|^2 + \left| \delta^N \right|^2 + \frac{2}{c_1} \left| \Delta_{1t}^N \right|^2 \right\} ds \\ + \int_0^t \left\{ \frac{c_1}{2} \left| D^2 z^N(s) \right|^2 + \left| z_t^N(s) \right|^2 \right\} ds. \end{aligned}$$

Defining

$$v^N(t) \equiv |z_t^N(t)|^2 + \frac{c_1}{2} |D^2 z^N(t)|^2$$

and

$$F^N(t) \equiv \frac{2}{c_1} |\Delta_1^N(t)|^2 + \int_0^t \left\{ \frac{1}{2c_2} |\Delta_{2t}^N|^2 + |\delta^N|^2 + \frac{2}{c_1} |\Delta_{1t}^N|^2 \right\} ds,$$

we have obtained

$$v^N(t) \leq F^N(t) + \int_0^t v^N(s) ds.$$

An application of the Gronwall inequality yields $v^N(t) \rightarrow 0$ if we can argue $F^N(t) \rightarrow 0$ for each t . But since $z^N(t) \in H_*^2$, the convergence $v^N(t) \rightarrow 0$ actually yields $z^N(t) \rightarrow 0$ in H_*^2 which in turn yields the desired convergence.

To complete the arguments, one recalls the definition of δ^N and Δ_i^N . Under assumptions (2.9) and the compactness of Q in \mathcal{L} (i.e., $q^N \rightarrow q$ in \mathcal{L}), the arguments for $F^N(t) \rightarrow 0$ can readily be reduced to smoothness requirements on $u = u(q)$ (e.g., $u, u_t \in L_2(0, T; H_*^2)$, $u_{tt} \in L_2(0, T; L_2)$). These in turn can be established as indicated above under additional smoothness hypotheses on the data (e.g., u_0, v_0, q, f) in our problem.

3. Implementation and Computational Considerations.

We next discuss implementation of schemes for the sequence of approximate estimation problems involving the systems (2.12) - (2.14) and criteria (2.15). This involves Ritz-Galerkin type procedures embedded in optimization routines. For these one needs state approximation subspaces H^N and parameter approximation sets Q^M . In the case of the work reported on in this paper, we employed subspaces H^N generated by either cubic or quintic B-splines appropriately modified to satisfy the essential or geometric boundary conditions (2.2) of $V = H_*^2(0,1)$ (or the analogs of these conditions in the event we are considering some other type of boundary condition, e.g. simply-supported, or tip appendage). We have used either linear or cubic interpolatory splines to define the sets Q^M . Once approximation sets H^N and Q^M have been chosen the equations (2.12) reduce to matrix differential equations for the "Fourier" coefficients of u^N relative to the basis elements for H^N and Q^M .

To illustrate the ideas in a specific case, we consider cubic spline state approximations and linear spline parameter approximation sets for a cantilevered damped beam modeled by (2.1)-(2.6).

We first describe construction of the basis elements for H^N . For a positive integer N and partition $\Delta^N = \{x_i\}_{i=0}^N$, $x_i = i/N$, of $[0,1]$, we denote by $S^3(\Delta^N)$ the set of cubic splines with knots Δ^N (i.e., the set of functions s such that s is a cubic polynomial on each interval (x_i, x_{i+1}) and is C^2 on $[0,1]$). Let $\{\hat{B}_i^N\}_{i=-1}^{N+1}$ be the standard cubic B-spline basis set for $S^3(\Delta^N)$ - see, for example [24, p. 79]. The cubic B-spline \hat{B}_i^N has support in (x_{i-2}, x_{i+2}) ,

has values 1, 4, 1 and slopes $1/N, 0, -1/N$ at the knots x_{i-1}, x_i, x_{i+1} respectively. The set $S^3(\Delta^N)$ is not contained in H_*^2 but we use the elements \hat{B}_j^N to generate basis elements B_j^N , that satisfy $B_j^N(0) = DB_j^N(0) = 0$. More precisely, we define

$$B_1^N = \hat{B}_0^N - 2\hat{B}_1^N - 2B_{-1}^N$$

$$B_i^N = \hat{B}_i^N, \quad i = 2, 3, \dots, N+1$$

and take $H^N = \text{span}\{B_1^N, B_2^N, \dots, B_{N+1}^N\}$.

Remark: When considering the clamped-free beam with tip mass, we choose

$$H^N = \text{span}\{\beta_1^N, \beta_2^N, \dots, \beta_{N+1}^N\}$$

$$\beta_j^N = (B_j^N(1), B_j^N), \quad j = 1, 2, \dots, N+1.$$

To construct Q^M for a positive integer M , we let $L(\Delta^M)$ be the set of piecewise linear splines [26, p. 10; 24, p. 48] corresponding to the partition $\Delta^M = \{i/M\}_{i=0}^M$. Basis elements for this set are given by the standard "hat" functions b_i^M , $i = 0, 1, \dots, M$ where b_i^M has support in (x_{i-1}, x_{i+1}) with values 0, 1, 0 at x_{i-1}, x_i, x_{i+1} respectively. Letting i_M denote the usual interpolation operator for $L(\Delta^M)$ - see [26, p. 10], we then define for a given Q , the approximation set $Q^M = i_M(Q)$. Note that in this particular case, the constraints $c_i \leq q_i(x) \leq v$ are preserved in Q^M .

We thus have that any solution $u^N(t) \in H^N$ of (2.12) has the representation

$$(3.1) \quad u^N(t, x) = \sum_{j=1}^{N+1} w_j^N(t) B_j^N(x)$$

while the coefficients q_1, q_2 to be chosen from Q^M have the representation

$$(3.2) \quad q_i^M(x) = \sum_{j=0}^M q_{ij} b_j^M(x).$$

For these fixed bases (for given indices (N,M)), it is easy to argue that (2.12) reduces to a second order $N+1$ dimensional system for $\hat{w}^N = (w_1^N, \dots, w_{N+1}^N)^T$. Specifically, (2.12) must hold for each $\psi = B_k^N$, $k = 1, \dots, N+1$; this, in view of the representation (3.1), yields an $N+1$ system of second order ordinary differential equations which can be rewritten as a $2N+2$ first order system

$$(3.3) \quad \begin{aligned} Q^N \dot{w}^N(t) &= K^N w^N(t) + f^N \\ Q^N w^N(0) &= w_0^N \end{aligned}$$

where now $w^N = (w_1^N, \dots, w_{2N+2}^N)^T$ with $w_{i+N+1}^N \equiv \dot{w}_i^N$, $i = 1, 2, \dots, N+1$, and

$$Q^N = \begin{bmatrix} I & 0 \\ 0 & Q_2^N \end{bmatrix}, \quad [Q_2]_{i,j} = \int_0^1 B_i^N B_j^N,$$

$$K^N = \begin{bmatrix} 0 & I \\ K_1^N(q_1) & K_1^N(q_2) \end{bmatrix}, \quad [K_1^N(q_\ell)]_{i,j} = \int_0^1 q_\ell D^2 B_i^N D^2 B_j^N,$$

$$f^N = \begin{bmatrix} 0 \\ f_2^N \end{bmatrix}, \quad [f_2^N]_j = \int_0^1 f B_j^N,$$

$$[w_0^N]_j = \int_0^1 u_0 B_j^N, \quad j = 1, \dots, N+1,$$

$$[w_0^N]_j = \int_0^1 v_0 B_{j-N-1}^N, \quad j = N+2, \dots, 2N+2.$$

The approximate estimation problems (for given integers N, M) thus reduce to minimization of

$$(3.4) \quad \phi^{N,M}(\tilde{q}) = \sum_{i,j} |u^N(t_i, x_j; q^M) - \tilde{u}_{ij}|^2$$

subject to (3.1), (3.2), (3.3) where now \tilde{q} is the vector of parameters q_{ij} in (3.2). For each set of fixed indices N, M , this problem can be successfully treated with a number of different techniques. We proceed to outline some of those which we have used. First, however, we note that computation of $\phi^{N,M}$ in any optimization routine requires solution of the semi-discrete Galerkin equations (3.3). This can be accomplished by using the Hindmarsh adaptation of the Gear algorithm [17]. For problems where $q_2(x) \equiv 0$ (no damping), the equations can be integrated efficiently using the Adams methods which are part of that scheme; however when damping is present the equations are stiff and we found it necessary to use the routines for stiff systems that are part of the Gear algorithm.

The evaluation of $\phi^{N,M}$ is the expensive part of our algorithms, involving the integration of moderately stiff systems of $2N+2$ dimensional differential equations. Some computational savings can be achieved due to the special structure of the matrices in (3.3): sparse, banded, with symmetry in the matrices Q_2^N and K_1^N . A Cholesky algorithm can be used at each integration step to solve for the $N+1$ subsystem involving Q_2^N . Elements of Q^N and K^N can be readily evaluated using a composite two-point Gaussian quadrature.

We have used, in the results reported herein and in earlier efforts [5], three different methods (sometimes in a hybrid scheme involving two of them) to carry out the minimization for $\phi^{N,M}$ in (3.4): (i) a finite-difference Levenberg-Marquardt (FDM) algorithm; (ii) a conjugate-gradient (CG) algorithm; and (iii) the scheme due to Broyden-Fletcher-Goldfarb-Shanno (BFGS). We describe each briefly below, referring the reader to the references given below for further details. We first note that (i) requires only evaluation of $\phi^{N,M}$ since derivative information is obtained by finite differences; methods (ii) and (iii) require gradients which we have computed using a costate equation approach (explained below).

(i) Finite-difference Levenberg-Marquardt: This quasi-Gauss-Newton [23] method is designed especially for minimization of least-squares criteria. Rewriting $\phi^{N,M}(\tilde{q})$ of (3.4) as $\sum_{\ell=1}^K e_{\ell}(\tilde{q})^2$ where $e(\tilde{q}) = (e_1(\tilde{q}), \dots, e_K(\tilde{q}))$ is the vector of residuals or pointwise errors, the L-M scheme generates a sequence of iterates

$$(3.5) \quad \tilde{q}^{(k+1)} = \tilde{q}^{(k)} + \lambda_k \tilde{d}^{(k)}$$

where the directions $\tilde{d}^{(k)}$ are obtained by solving

$$(3.6) \quad (J_k^T J_k + \mu_k I) \tilde{d}^{(k)} = -J_k^T e(\tilde{q}^{(k)})$$

with the scalar μ_k chosen to insure positive definiteness of the system matrix in (3.6) and so that $\tilde{d}^{(k)}$ is a descent direction. Here the matrix J_k is the Jacobian matrix of $e(\tilde{q})$ evaluated at $\tilde{q}^{(k)}$. For $\mu_k = 0$ the directions thus obtained agree with those of the Gauss-Newton method while for μ_k large the directions approach those of steepest descent.

This method generates descent directions and exhibits rapid convergence (superlinear). However, to approximate the Jacobian in (3.6) by finite differences (which is the standard approach for this method), the differential equations (3.3) must be integrated p times, where p is the number of parameters in the vector $\tilde{q} = (q_{ij})$. Thus at each iteration of (3.5), the approximating differential equations must be solved p times to generate one descent direction. This is not a significant drawback if p is not too large. For spatially varying stiffness and damping coefficients q_1, q_2 in (2.1), the total number of parameters needed to obtain reasonable approximations can become large. In this event alternate methods may be superior.

One can avoid methods based on finite-difference gradients if one is willing to compute the necessary gradients (e.g., by variational equations or costate methods) and supply them directly to the iterative algorithm. While there is a version of the Levenberg-Marquardt algorithm (in MINPACK's LMSTR1) which allows user calculated gradients, we have chosen to investigate use of other popular algorithms in some of the calculations we have carried out. Since the use of linear variational equations in calculating the gradients involves solving systems that grow in dimension with the number of sought-after parameters (p in the discussion above), we have chosen to use a costate formulation in computing gradients. In this case only two differential equations (with dimension independent of the number of parameters to be estimated) must be integrated per iteration. The associated iterative algorithms we have used are the conjugate-gradient and the BFGS.

(ii) Conjugate-Gradient: The CG algorithm is quite well-known (see [16, p. 133-136; 15, p. 91-98] for more details) and we use the formulation proposed by Nazareth in [21]. Once again the iterates are given by (3.5) but the directions are generated by the recurrence relationships

$$d^{(0)} = 0$$

$$d^{(1)} = -g^{(1)}$$

$$d^{(k+1)} = -y^{(k)} + (y^{(k-1)T} y^{(k)} / y^{(k-1)T} d^{(k-1)}) d^{(k-1)} \\ + (y^{(k)T} y^{(k)} / y^{(k)T} d^{(k)}) d^{(k)}$$

where $y^{(k)} = g^{(k+1)} - g^{(k)}$ with $g^{(k)}$ the gradient vector (of $\phi^{N,M}$ with respect to the parameters \tilde{q}) evaluated at $\tilde{q}^{(k)}$.

While CG methods exhibit finite-step convergence when the cost criterion is a quadratic functional, in general problems such as those under investigation here convergence is often slow, particularly in the neighborhood of the extremal point. Newton methods are more suitable near the extremal and hence it is often advantageous to switch to a quasi-Newton method such as the BFGS.

(iii) Broyden-Fletcher-Goldfarb-Shanno: In this method one again uses the iterative formula (3.5) with the search directions $\tilde{d}^{(k)}$ now given by

$$\tilde{d}^{(k)} = -H^k g^{(k)}$$

where $g^{(k)}$ again denotes the gradient and

$$\begin{aligned}
 H^{k+1} &= H^k + (1 + \gamma_k^T H^k \gamma_k / \delta_k^T \gamma_k) \delta_k \delta_k^T / \delta_k^T \gamma_k \\
 &\quad - (\delta_k \gamma_k^T H^k + H^k \gamma_k \delta_k^T) / \delta_k^T \gamma_k, \\
 \delta_k &\equiv \tilde{q}^{(k+1)} - \tilde{q}^{(k)}, \quad \gamma_k \equiv g^{(k+1)} - g^{(k)}, \\
 H^0 &= I.
 \end{aligned}$$

This quasi-Newton method employs "BFGS updates" H^k for a matrix which is an approximation to the inverse Hessian matrix. In practice, the method exhibits rapid convergence for the type of problems we have considered, particularly when compared to the CG method (ii) in the neighborhood of an extremum. Second order information is used (i.e., an approximate inverse Hessian matrix) even though only gradient computations are required. In our implementations, the gradient is computed using a costate formulation and hence as in the case of the CG method, only two differential equation solutions (state and costate) are required per step, as compared to the FDLN (or any other finite-difference based gradient algorithm) which requires p (= dimension of unknown parameter vector) differential equations be solved per step.

The step parameter λ_k is determined by a one-dimensional line search, with the BFGS and CG methods offering the advantage that exact line searches are not necessary. For a further discussion of the BFGS method, the reader may consult [15, p. 38-60].

The method of using costates to compute the gradient in optimization problems with differential equation constraints is well-known to investigators in control and variational theory. These ideas in a form appropriate

for parameter estimation problems are described in some detail by Chavent [12] for the case of continuous time observation problems. A similar formulation for discrete time criteria such as (3.4) can be given. We refer the reader to the Appendix where it is shown that the desired gradients are given by

$$\frac{\partial \phi^{N,M}}{\partial q_{ij}}(\tilde{q}) = - \int_0^T p^T(t) \mathcal{H}_{ij} w^N(t) dt$$

with

$$\mathcal{H}_{1j} = \begin{bmatrix} 0 & 0 \\ \mathcal{D}_j & 0 \end{bmatrix}$$

$$\mathcal{H}_{2j} = \begin{bmatrix} 0 & 0 \\ 0 & \mathcal{D}_j \end{bmatrix}, \quad j = 0, 1, \dots, M,$$

where \mathcal{D}_j is the $N \times N$ matrix with elements

$$[\mathcal{D}_j]_{i,k} = \int_0^1 b_j^M D^2 B_i^N D^2 B_k^N dx$$

and p satisfies an appropriately defined costate (to (3.3)) equation (see (A.7) in the Appendix).

4. Numerical Results and Examples

We have developed and tested software packages based upon both quintic and cubic spline state approximations and cubic and linear spline parameter approximations as noted above (some of our findings were reported in an earlier version of this paper [5]). Numerical testing was carried out on a CDC Cyber 173 at NASA Langley Research Center, a Burroughs 6900 at the USAF Academy, and an IBM 3081 at the University of Southern California. The IMSL version of the Gear/Hindmarsh algorithm (DGEAR) was used to integrate the approximating differential equations (3.3). One of several methods was used to solve the approximating optimization problems: the IMSL implementation ZXSSQ of the Levenberg-Marquardt algorithm, the BFGS scheme or a hybrid CG/BFGS scheme (i.e., initially using the CG algorithm and switching to the BFGS as we neared a minimizer).

To test the approximation ideas, the inverse procedure, and software, synthetic data was generated for a number of examples in the following manner: "true" parameter functions q_1^* , q_2^* were chosen and an algorithm employing either finite differences or a high order spline based Galerkin scheme was used to generate the corresponding solution values $\tilde{u}_{ij} = u(t_i, x_j; q^*)$ at certain points (t_i, x_j) on a grid. These values (which obviously already contain some "noise") were subsequently used as observations or input for the estimation algorithms and software being tested.

A number of test examples with different shaped stiffness and damping functions were investigated in this manner. We report in this section some of these results. The results we summarize are typical of our numerical findings. Each of the particular examples detailed below was run using the ZXSSQ package, although we have also enjoyed success with

the other optimization methods discussed above (e.g., see [5] where some of the results given were obtained using the CG and BFGS schemes).

In Examples 1 and 2 below, for "true" parameter functions q_1^* , q_2^* , "data" was generated using a finite difference scheme for observation points (t_i, x_j) with $t_i = i/10$, $x_j = j/10$, $i, j = 1, 2, \dots, 10$. The test model equation used is given by (2.1) - i.e.,

$$(4.1) \quad u_{tt} + D^2\{q_1 D^2 u + q_2 D^2 u_t\} = f, \quad 0 < x < 1,$$

with initial data $u(0, x) = u_t(0, x) \equiv 0$ and uniform loading $f(t, x) \equiv 10$.

The boundary conditions used were for a simply supported beam, that is,

$$(4.2) \quad u(t, 0) = u(t, 1) = D^2 u(t, 0) = D^2 u(t, 1) = 0.$$

In the results reported below, the index N will always refer to the state approximation level with either N+1 quintic basis elements (note this is a strong formulation with all four conditions of (4.2) imposed on the basis elements) or N+1 cubic basis elements (a weak formulation in which the zero moment conditions are treated as natural boundary conditions). Similarly the index M will denote the parameter approximation index with M+1 linear splines or M+3 cubic splines in a basis set.

In carrying out the optimization step, it was often necessary to impose the pointwise positivity constraint $q_1(x) \geq c_1 > 0$ of \tilde{Q} on the stiffness estimate $q_1^{N,M}$ generated by the various schemes. We denote by $\hat{q}_i^{N,M}$ the converged parameter estimates (to be compared with q_i^* , the true parameter functions) and tabulate one or more of the following measures of performance:

$$(4.3) \quad \hat{\phi}^{N,M} \equiv \sum_{i,j} |u^N(t_i, x_j; \hat{q}^{N,M}) - \tilde{u}_{ij}|^2$$

$$(4.4) \quad E_i^{N,M} \equiv |q_i^* - \hat{q}_i^{N,M}|$$

where $|\cdot|$ in (4.4) denotes the norm in $L_2(0,1)$.

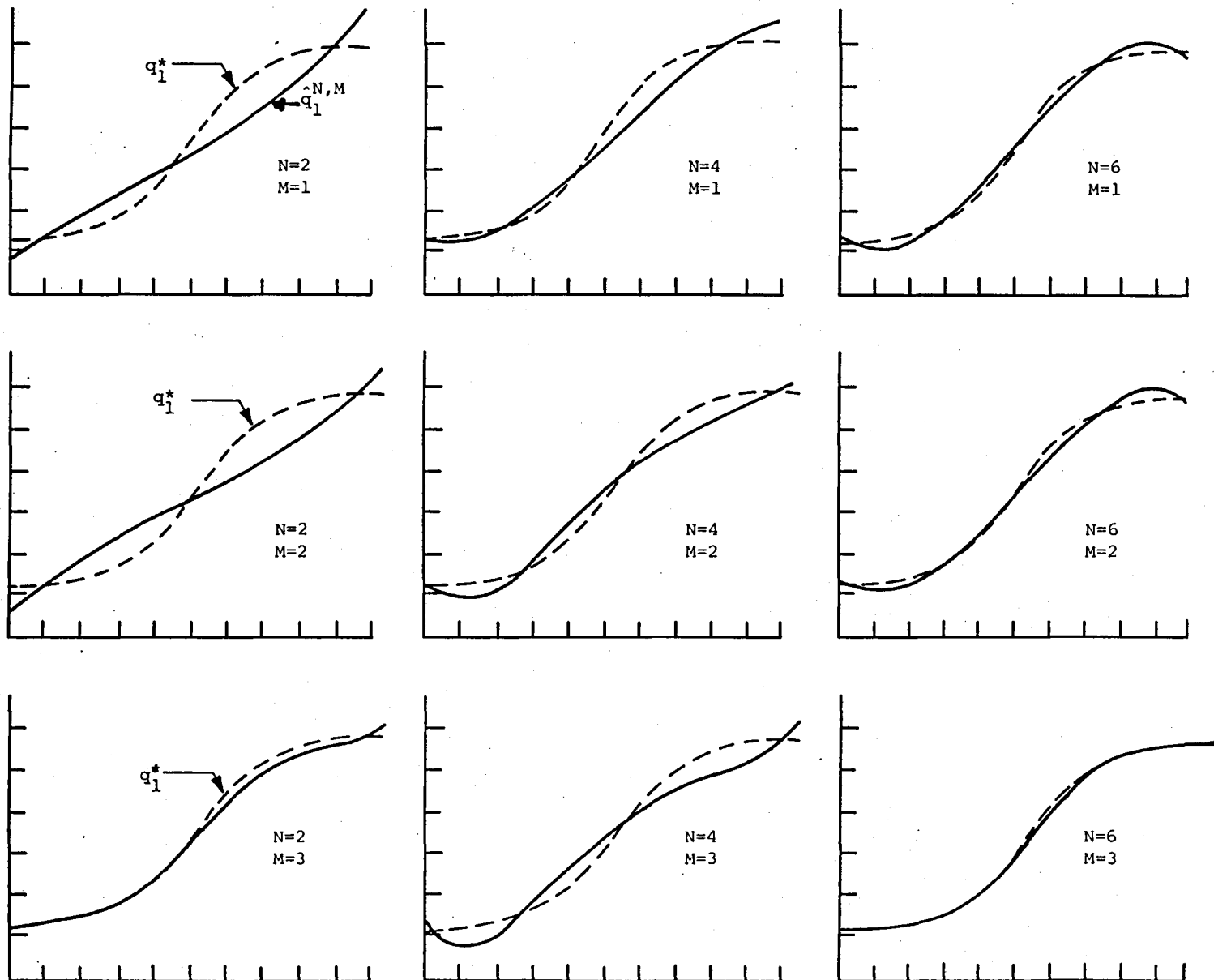
Example 1. We consider an undamped beam ($q_2^* \equiv 0$) with stiffness $q_1^*(x) = .15 + .10 \tanh[5(x-.5)]$. We estimate q_1 from start-up value $q_1^0 \equiv .15$ using quintic spline state approximations, and cubic spline parameter approximations. In Figure 4.1 we present a graphical record of the convergence $\hat{q}_1^{N,M} \rightarrow q^*$ while in Table 4.1 we list the corresponding values for $\hat{\phi}^{N,M}$ and $E_1^{N,M}$. In all of our graphs, the true parameter functions are represented with dashed curves while the estimates $\hat{q}_1^{N,M}$ are given by a solid curve.

		<u>N=2</u>	<u>N=4</u>	<u>N=6</u>
M=1	$\hat{\phi}^{N,M}$	$.21 \times 10^{-3}$	$.43 \times 10^{-4}$	$.20 \times 10^{-4}$
	$E_1^{N,M}$.0207	.0106	.0055
M=2	$\hat{\phi}^{N,M}$	$.18 \times 10^{-3}$	$.13 \times 10^{-4}$	$.16 \times 10^{-4}$
	$E_1^{N,M}$.0213	.0115	.0060
M=3	$\hat{\phi}^{N,M}$	$.18 \times 10^{-3}$	$.91 \times 10^{-5}$	$.34 \times 10^{-5}$
	$E_1^{N,M}$.0048	.0146	.0010

TABLE 4.1

FIGURE 4.1

QUINTIC STATES/CUBIC PARAMETERS



Example 2. We consider the same example as in Example 1 except that we used $q_1^*(x) = .15 + .10 \tanh[20(x-.5)]$. Tests were conducted to compare the performance of our algorithms with quintic vs. cubic state approximations and cubic vs. linear parameter approximations. Typical values for $\hat{\phi}^{N,M}$ and $E_1^{N,M}$ are given in Table 4.2 along with some typical graphs in Figures 4.2 and 4.3. In tabulating the results, we use the labels (N,M,S,P) with state approximations given by

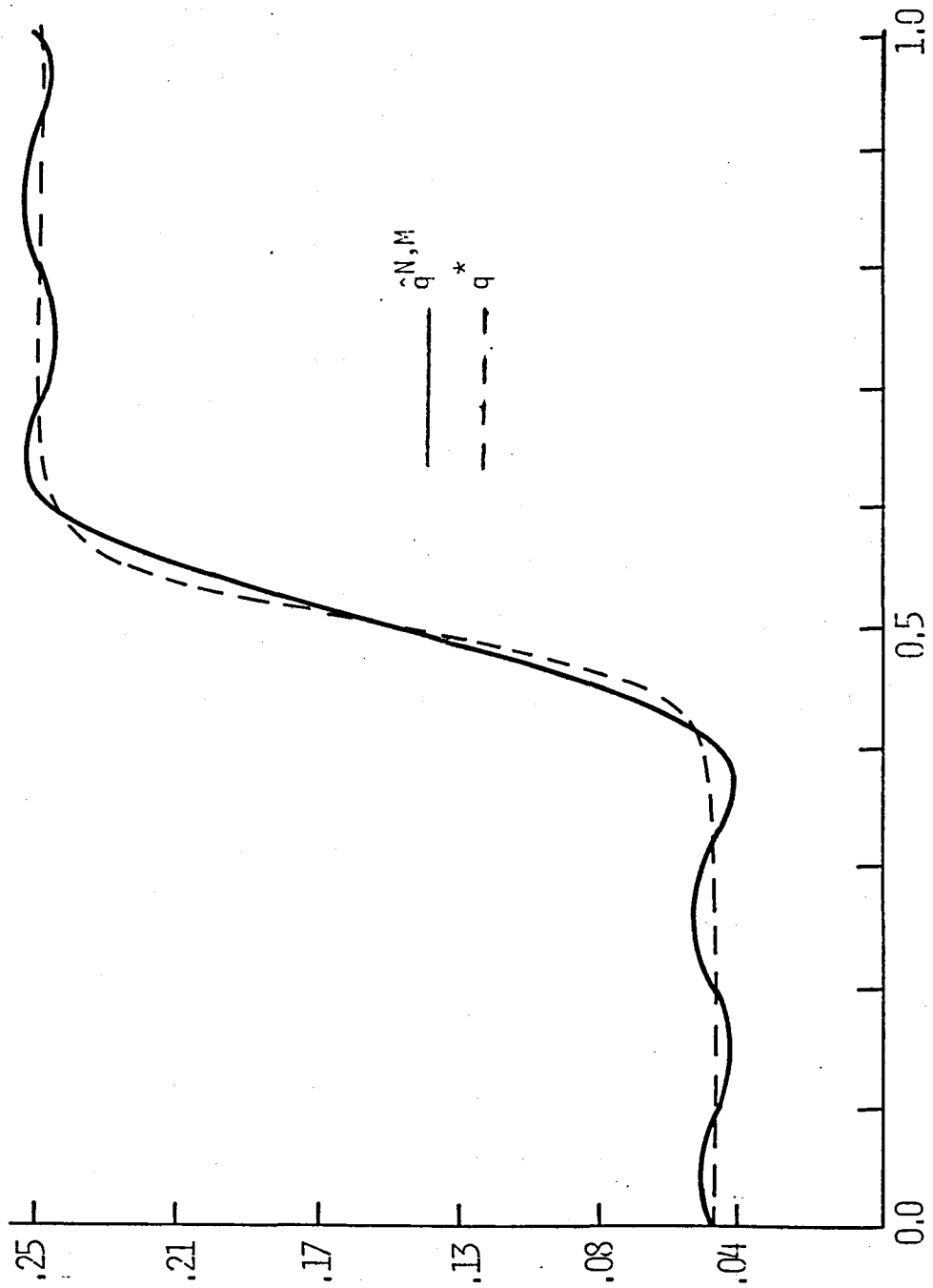
$S = Q$ (quintic) or $S = C$ (cubic)

and parameter approximations given by

$P = C$ (cubic) or $P = L$ (linear).

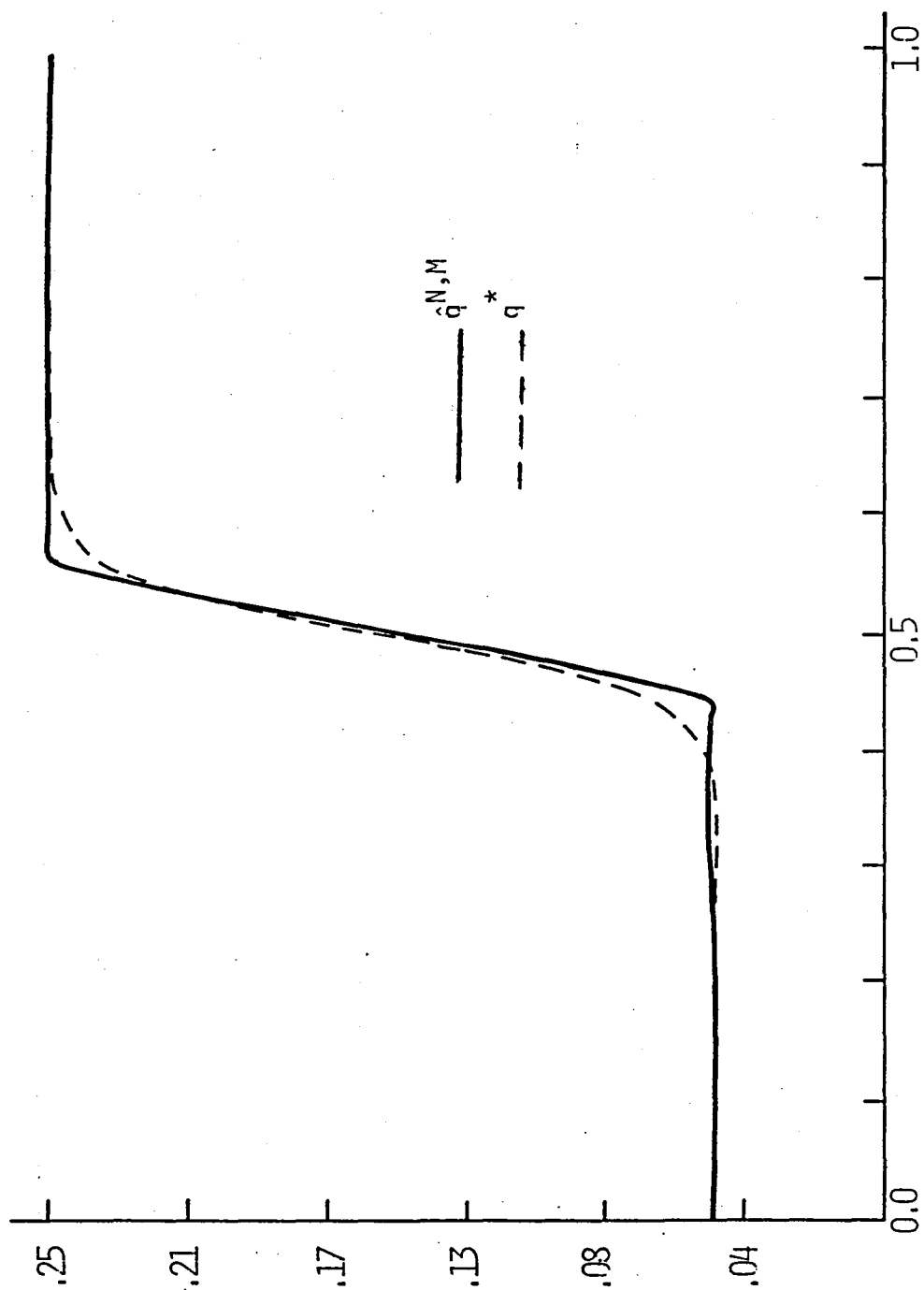
<u>(N,M,S,P)</u>	<u>$\hat{\phi}^{N,M}$</u>	<u>$E_1^{N,M}$</u>
(8,7,Q,C)	$.546 \times 10^{-6}$	$.86 \times 10^{-2}$
(8,7,Q,L)	$.302 \times 10^{-5}$	$.89 \times 10^{-2}$
(8,7,C,C)	$.241 \times 10^{-6}$	$.12 \times 10^{-1}$
(8,7,C,L)	$.224 \times 10^{-5}$	$.30 \times 10^{-2}$

TABLE 4.2



(12.7.C.C): $N = 12M = 7/\text{CUBIC STATES/CUBIC PARAMETERS}$

FIGURE 4.2



(8,9,C,L): $N=8/M=9$ /CUBIC STATES/LINEAR PARAMETERS

FIGURE 4.3

In Examples 3, 4 and 5 we consider a clamped-free or cantilevered beam with a variety of configurations at the free end, $x=1$. More precisely, in its most general form, we consider the beam with a rigidly attached tip body. The dynamics are given by the hybrid system of ordinary and partial differential equations (see [10], [28], [29], [30])

$$(4.5) \quad \rho u_{tt} + D^2\{q_1 D^2 u + q_2 D^2 u_t\} = D\{\sigma Du\} + f, \quad 0 < x < 1, \quad t > 0,$$

$$(4.6) \quad m u_{tt} + m c D u_{tt} - D\{q_1 D^2 u + q_2 D^2 u_t\} = -\sigma Du + g, \quad x=1, \quad t > 0,$$

$$(4.7) \quad m c u_{tt} + (J + m c^2) D u_{tt} + q_1 D^2 u + q_2 D^2 u_t = -c \sigma Du + h, \quad x=1, \quad t > 0,$$

$$(4.8) \quad u(t, 0) = 0, \quad D u(t, 0) = 0, \quad t > 0,$$

$$(4.9) \quad u(0, x) = u_0(x), \quad u_t(0, x) = v_0(x), \quad 0 < x < 1,$$

where $\rho=\rho(x)$ is the linear mass density of the beam, m is the mass of the tip body and J is its moment of inertia about its center of mass. The center of mass of the tip body is assumed to lie at a distance c from the tip of the beam directed along the tangent in the x -direction at the tip to the beam's neutral axis (see Figure 4.4 below).

The second order term $D\{\sigma Du\}$ in (4.5) and the corresponding terms in (4.6) and (4.7) are the forces and moments which result from an axial loading $\sigma=\sigma(t, x)$. In the examples below, we only consider axial loads

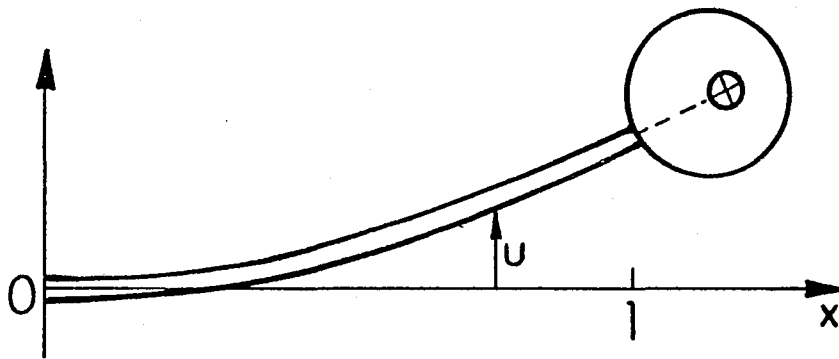


Figure 4.4

which result from an acceleration $a_0 = a_0(t)$ of the base of the structure in the positive x-direction. In this case, we have (see [10], [29], [30])

$$\sigma(t, x) = -a_0(t) \left\{ m + \int_x^1 \rho(y) dy \right\} .$$

The equations (4.6) and (4.7) represent respectively transverse and rotational equilibrium at the tip of the beam with $g = g(t)$ denoting an externally applied load through the center of mass of the tip body in the transverse direction and $h = h(t)$ an externally applied torque or moment.

Note that setting $\rho=1$, $m=J=c=0$ and taking $a_0=g=h=0$ in equations (4.5), (4.6) and (4.7) leads to the dynamical equations for the standard cantilevered beam treated in Section 2. In the examples which follow we set

$$f(t, x) = e^x \sin 2\pi t,$$

took "true" values for the unknown parameters and used a quintic-spline based Ritz-Galerkin method to integrate the system (4.5) - (4.9) and generate displacement observations at times $t_i = .2i$, $i=0,1,2,\dots,5$ at positions $x_j = .25j$, $j=2,3,4$ along the span of the beam. The structure was assumed to be initially at rest (i.e., $u_0=v_0=0$).

The modifications to the formulation of the approximation schemes and the associated convergence theory necessitated by the presence of the tip appendages were briefly described and summarized in remarks in Sections 2 and 3 above. A complete and detailed discussion of our general approach in the context of inverse problems involving hybrid systems describing the vibration of beams with tip bodies can be found in [10].

As might be apparent from the results of our numerical studies which will be presented below, clamped-free beams posed a somewhat stiffer challenge for our methods than did the simply-supported beams in the examples discussed previously. An inherent ill-posedness of the problem of estimating variable parameters in distributed systems was more evident here than when beams with simple boundary conditions were treated.

An undesirable behavior (early onset of oscillations in the parameter estimates) may have resulted in part from the fact that in general in the presence of "higher order" boundary conditions it is more difficult to obtain accurate approximating solutions to the dynamical equations.

Example 3. In this example we simultaneously estimate a constant stiffness coefficient, $q_1^* = .15$ and a variable damping coefficient,

$$q_2^*(x) = .01(1.5 - \tanh(20x - 10))$$

in a model of the form (4.5) - (4.9) for a cantilevered beam with no tip appendage (i.e., with $m = J = c = 0$). We took $\rho(x) = 3 - x$ and $a_0 = g = h = 0$. Start up values for the optimization routine were chosen as $q_1^0 = .10$ and

$$q_2^0(x) = .015, \quad 0 \leq x \leq 1.$$

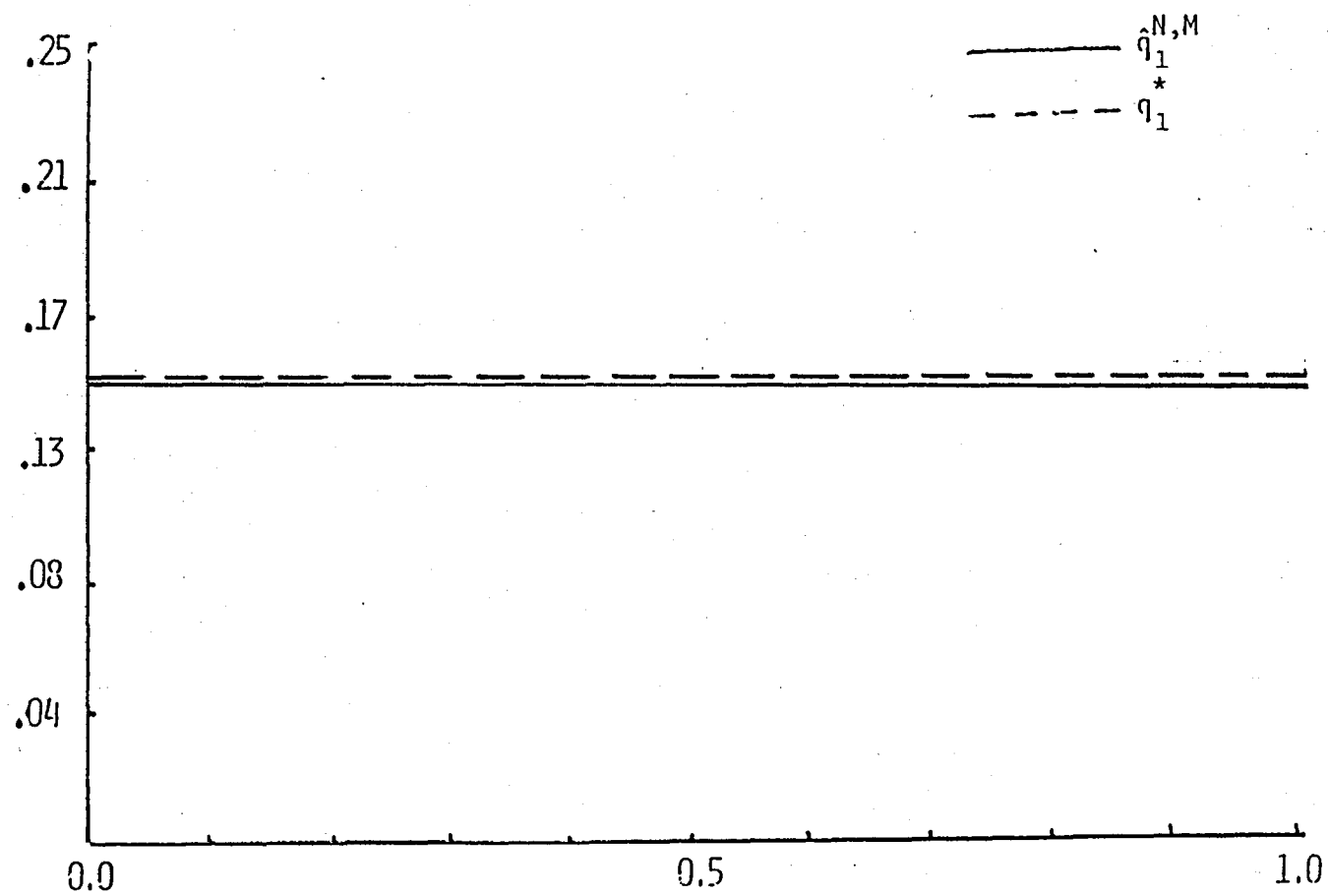
Since in this example we are simultaneously estimating two parameters, the parameter space discretization index M is in fact a vector, $M = (M_1, M_2)$ of two indices with M_i corresponding to the discretization for q_i , $i = 1, 2$.

Using five cubic splines for the state approximation ($N = 4$), two linear splines to discretize the stiffness coefficient ($M_1 = 1$) and four

linear spline elements to discretize the damping coefficient ($M_2 = 3$) we produced the estimates plotted in Figures 4.5 and 4.6. With eight cubic splines to discretize the damping coefficient ($M_2 = 5$, all other approximation parameters left unchanged) we produced the estimates plotted in Figures 4.7 and 4.8. Using the labeling convention $(N, M_1, M_2, S, P_1, P_2)$ we obtained

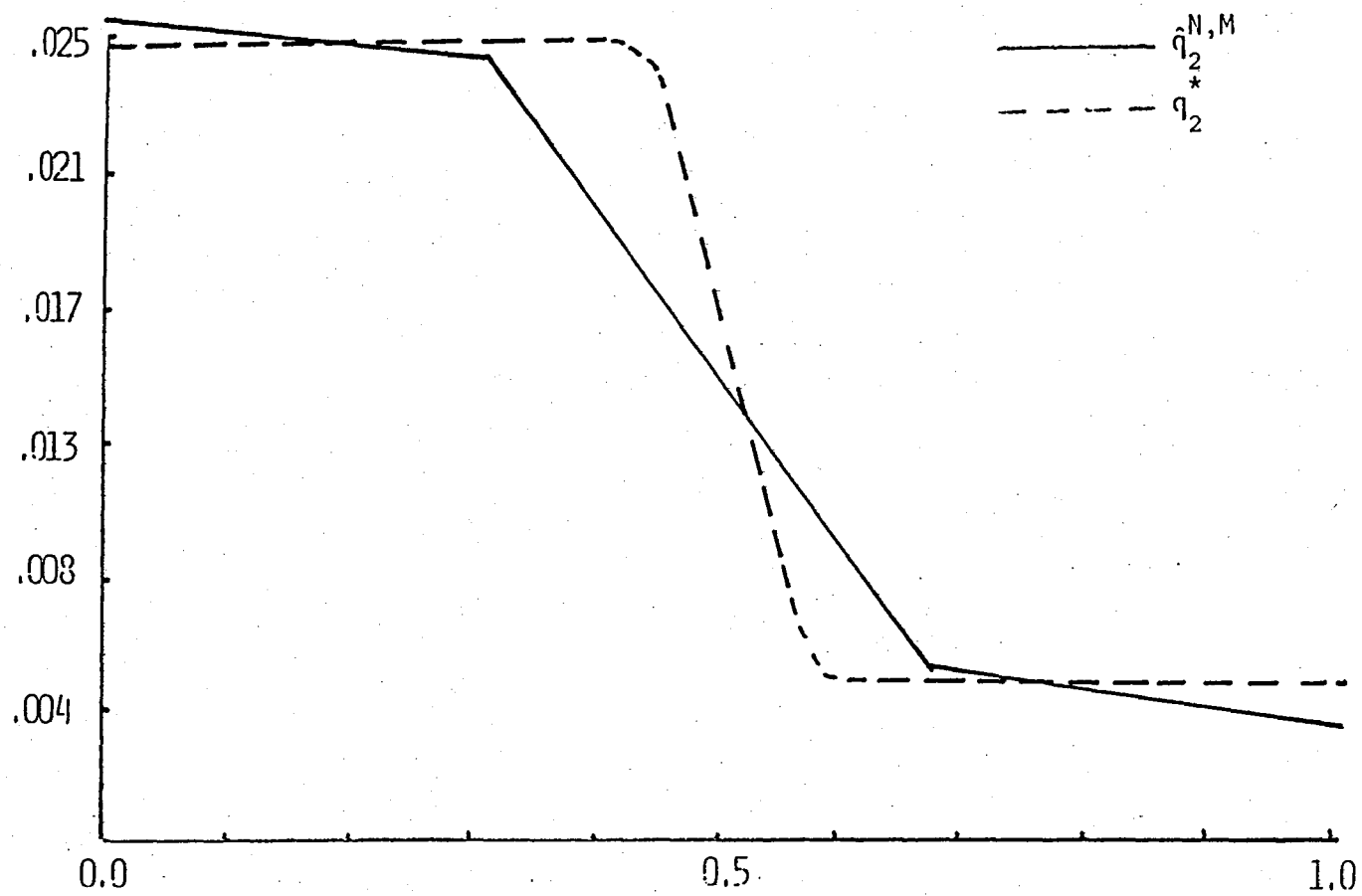
<u>$(N, M_1, M_2, S, P_1, P_2)$</u>	<u>$\hat{\phi}^{N, M}$</u>	<u>$E_1^{N, M}$</u>	<u>$E_2^{N, M}$</u>
$(4, 1, 3, C, L, L)$	$.377 \times 10^{-6}$	$.908 \times 10^{-3}$	$.210 \times 10^{-2}$
$(4, 1, 5, C, L, C)$	$.323 \times 10^{-6}$	$.414 \times 10^{-2}$	$.256 \times 10^{-2}$

The CPU times on the IBM 3081 for these two runs were 22.43 seconds and 29.92 seconds respectively.



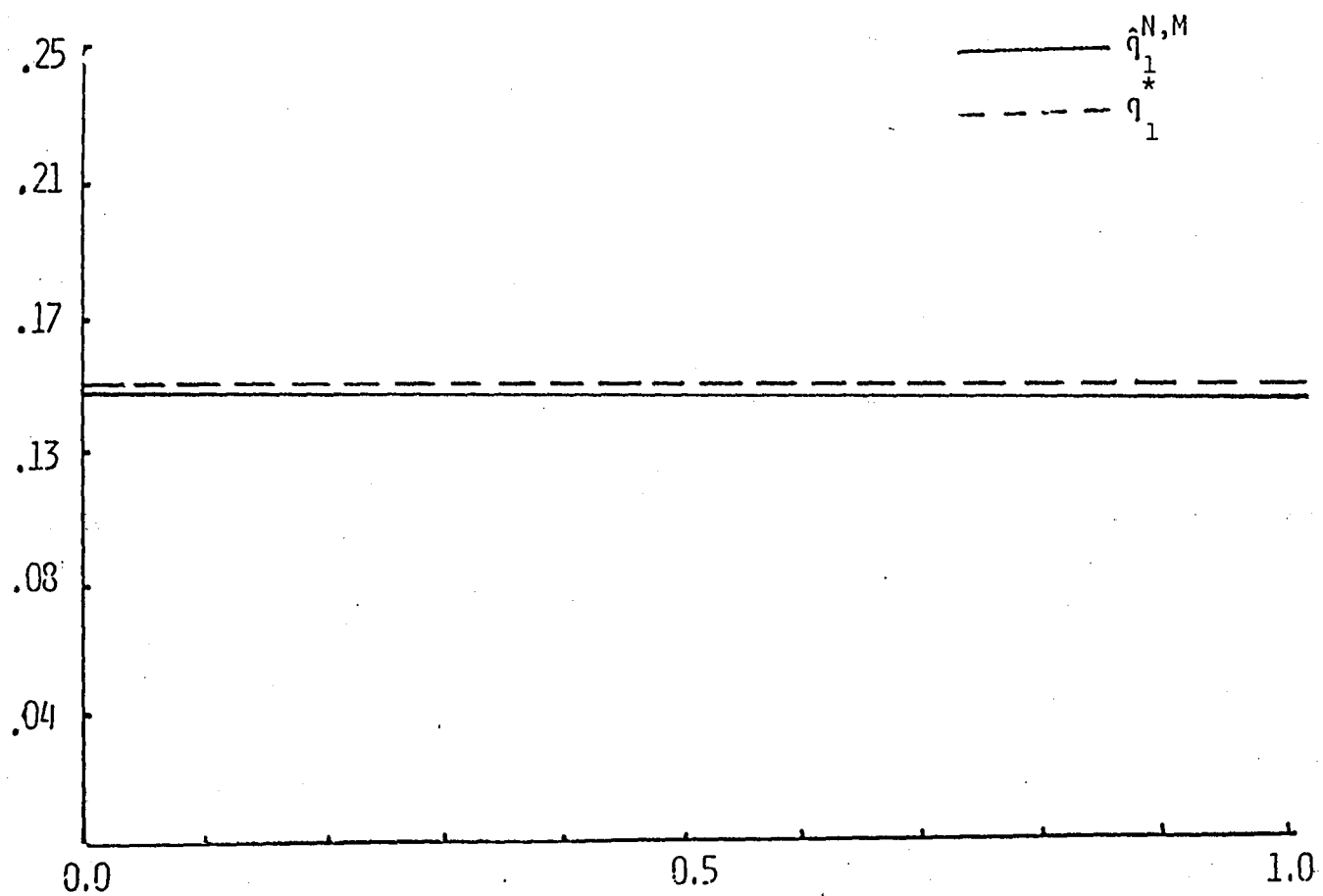
(4,1,3,C,L,L): $N=4/M_1=1/M_2=3$ /CUBIC STATES/LINEAR PARAMETERS/LINEAR PARAMETERS

FIGURE 4.5



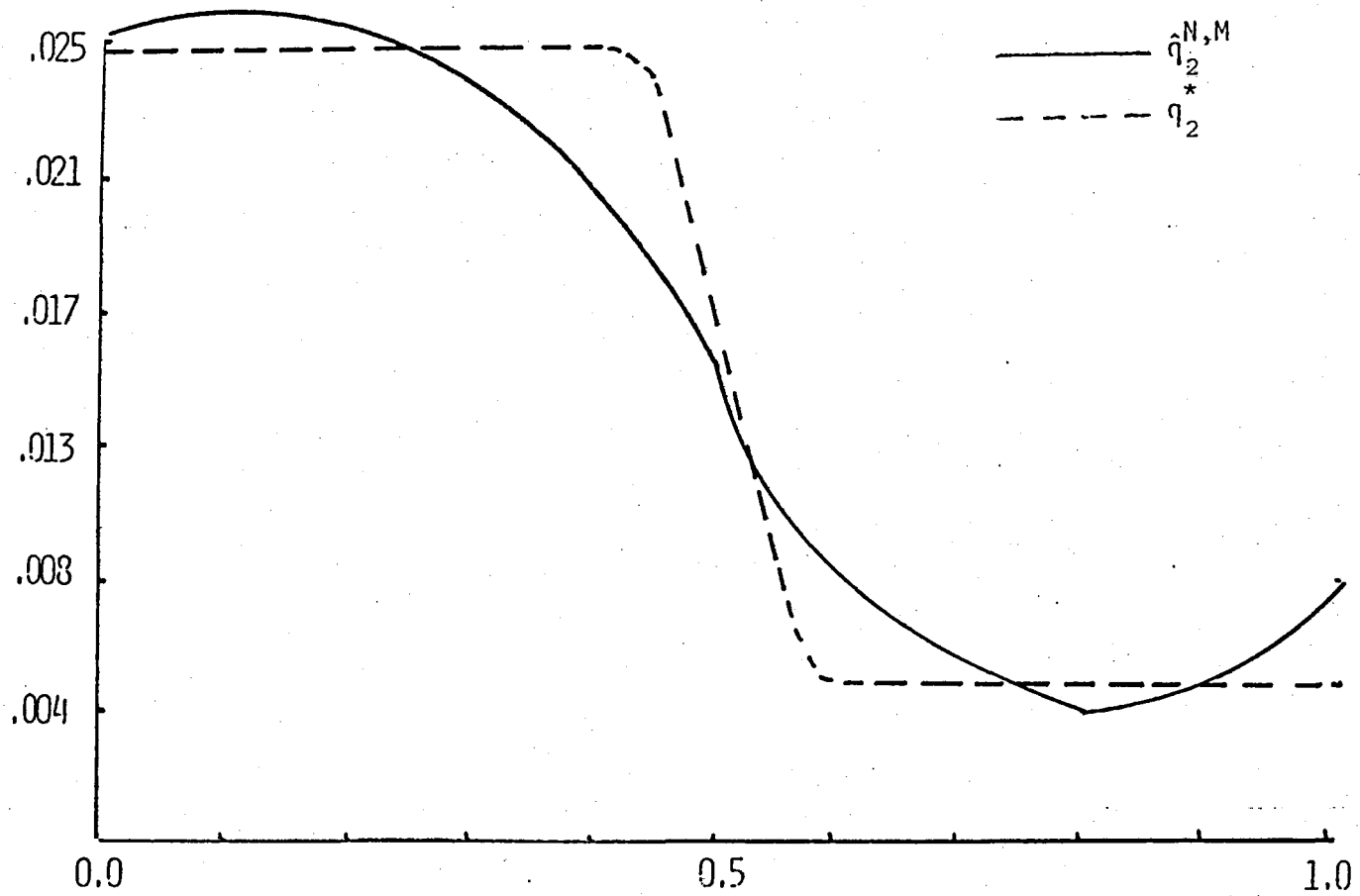
(4,1,3,C,L,L): $N=4/M_1=1/M_2=3$ /CUBIC STATES/LINEAR PARAMETERS/LINEAR PARAMETERS

FIGURE 4.6



(4,1,5,C,L,C): $N=4/M_2=1/M_2=5$ /CUBIC STATES/LINEAR PARAMETERS/CUBIC PARAMETERS

FIGURE 4.7



(4,1,5,C,L,C): $N=4/M_1=1/M_2=5$ /CUBIC STATES/LINEAR PARAMETERS/CUBIC PARAMETERS

FIGURE 4.8

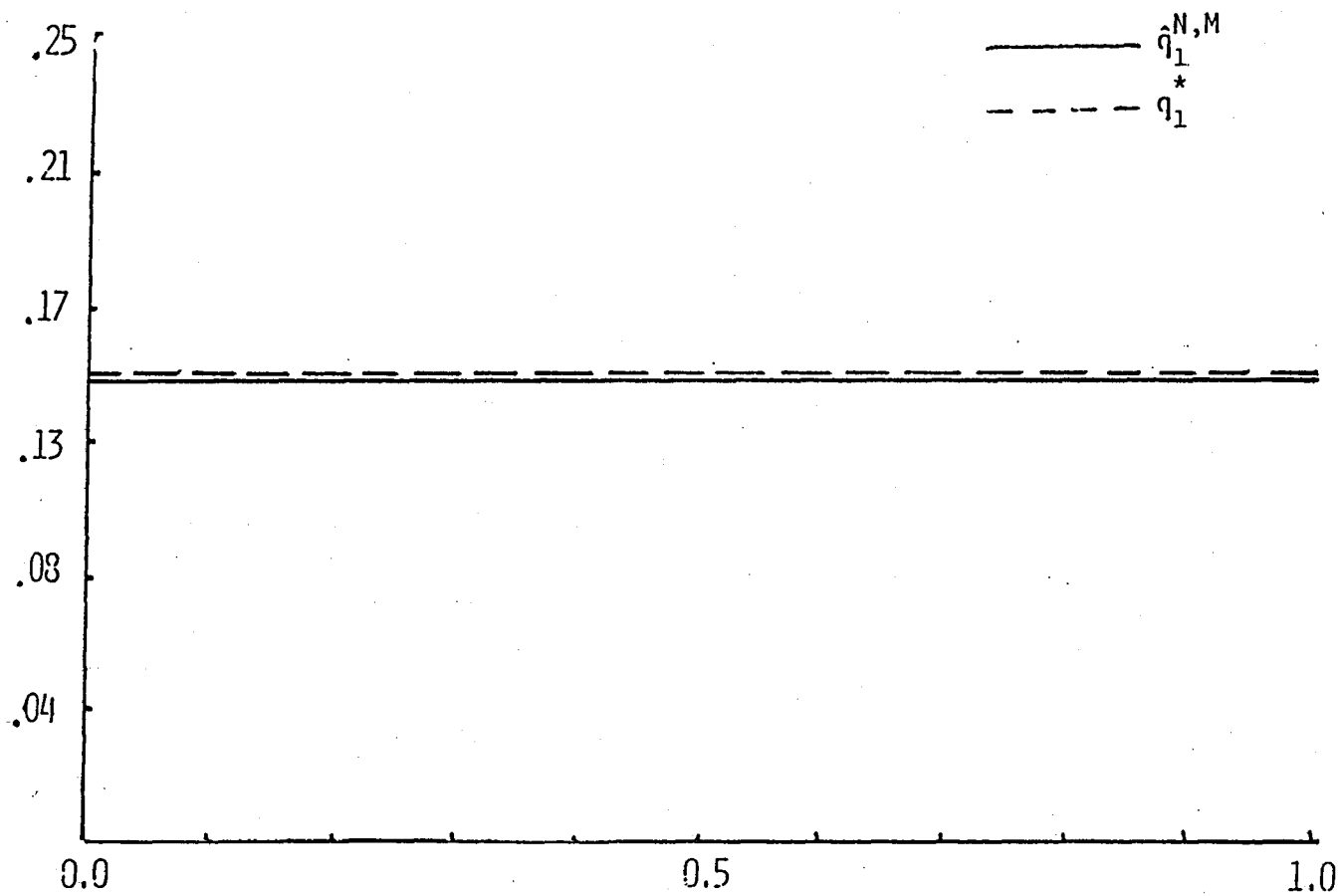
Example 4. We consider a cantilevered beam with a point ($c = J = 0$) mass of magnitude $m = 1.5$ rigidly attached to its free end. We took $a_0 = 1$, $g(t) = 2e^{-t}$ and $h(t) = e^{-2t}$. We simultaneously estimated a constant stiffness coefficient, $q_1^* = .15$ and a variable damping coefficient,

$$q_2^*(x) = .01(1.5 - \tanh(3x - 1.5)).$$

The start up values were taken to be $q_1^0 = .1$ and $q_2^0(x) = .015$, $0 \leq x \leq 1$.

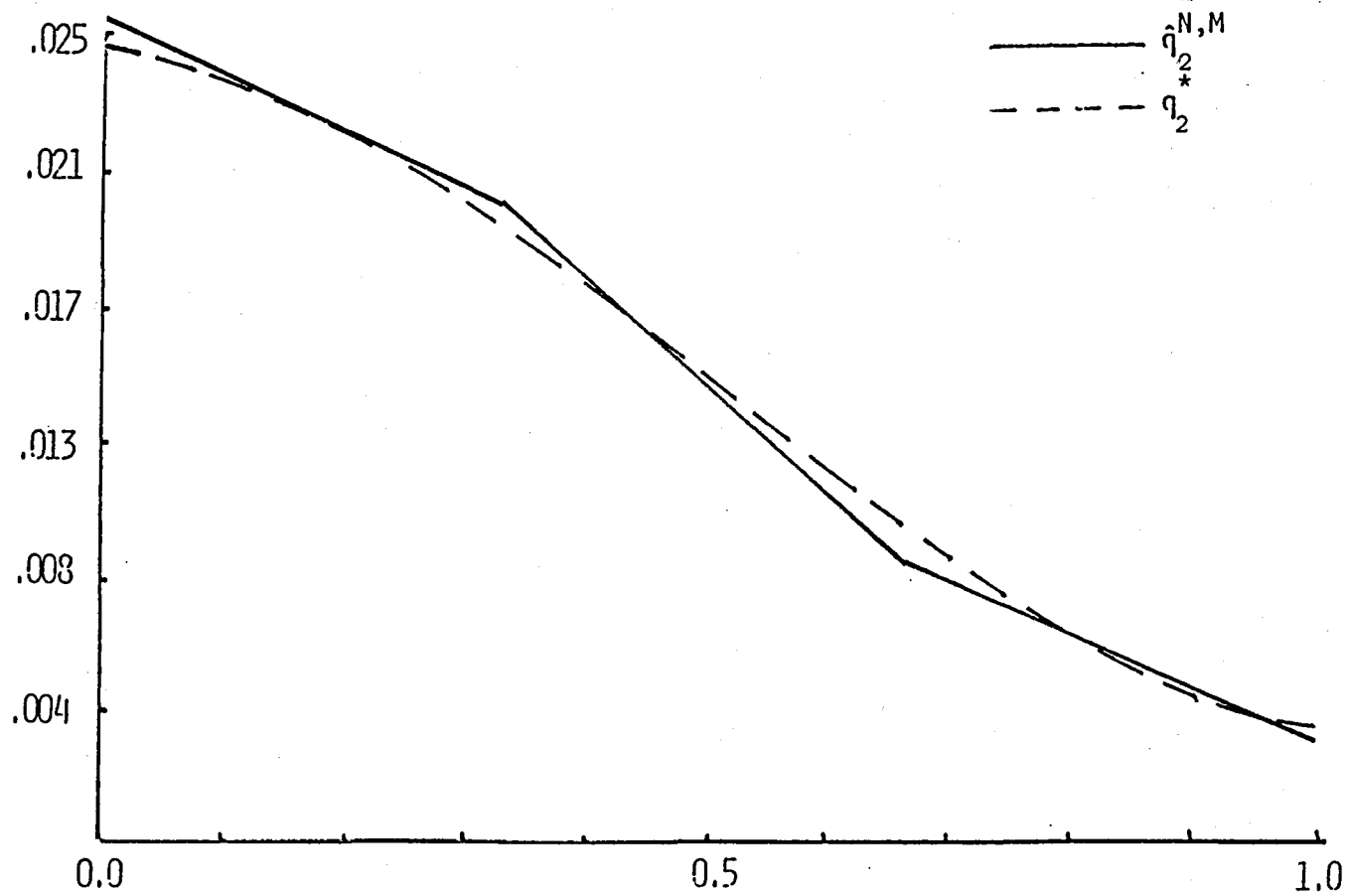
With a five cubic spline based state approximation ($N=4$), a two linear spline based discretization of the stiffness coefficient ($M_1 = 1$) and a four linear spline ($M_2 = 3$) or a five cubic spline ($M_2 = 2$) discretization of the damping coefficient we obtained the estimates plotted in Figures 4.9 - 4.12 with

$(N, M_1, M_2, S, P_1, P_2)$	$\hat{\phi}^{N,M}$	$E_1^{N,M}$	$E_2^{N,M}$
$(4, 1, 3, C, L, L)$	$.747 \times 10^{-7}$	$.669 \times 10^{-3}$	$.364 \times 10^{-3}$
$(4, 1, 2, C, L, C)$	$.404 \times 10^{-7}$	$.572 \times 10^{-3}$	$.702 \times 10^{-3}$



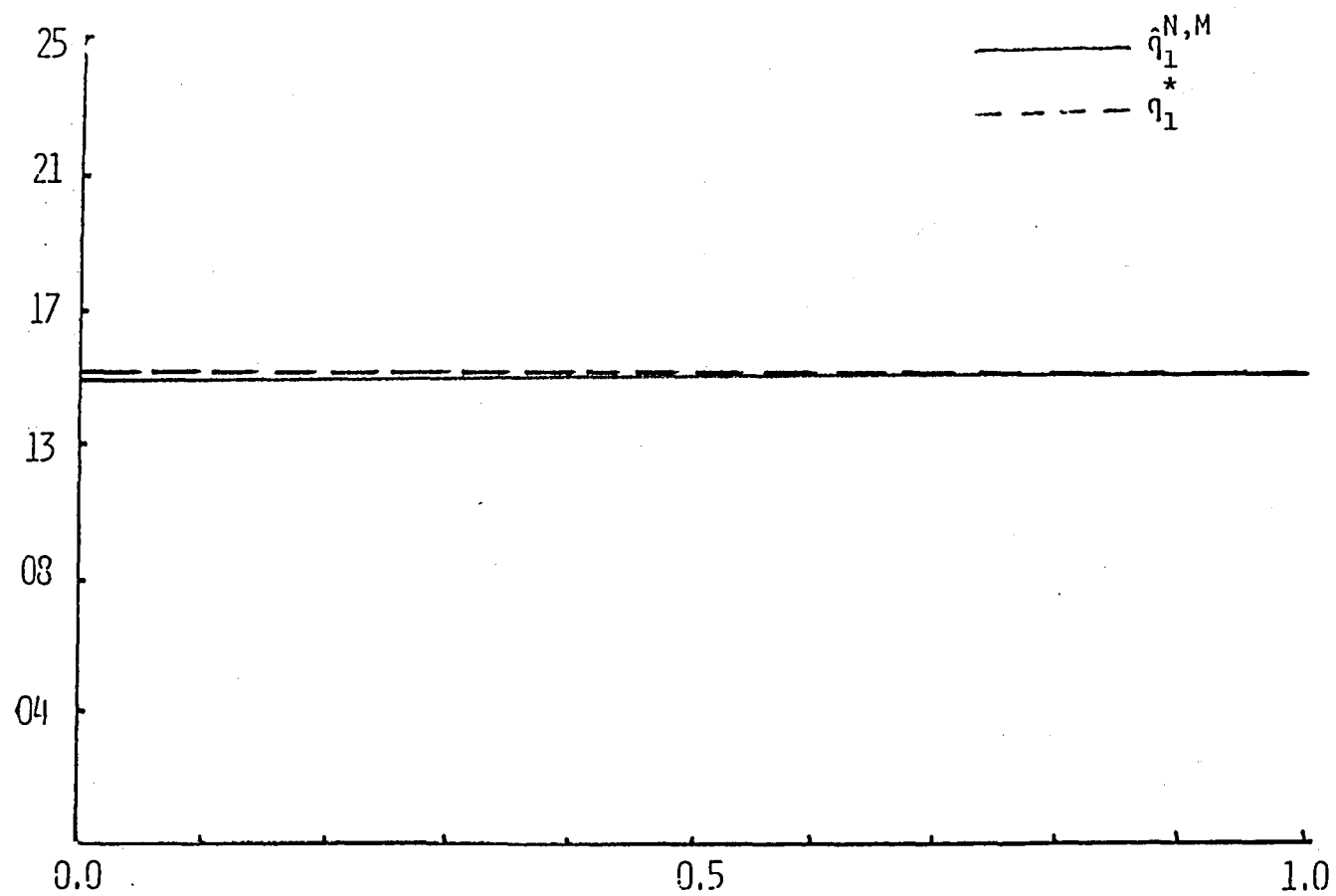
(4,1,3,C,L,L): $N=4/M_1=1/M_2=3$ /CUBIC STATES/LINEAR PARAMETERS/LINEAR PARAMETERS

FIGURE 4.9



(4,1,3,C,L,L): $N=4/M_1=1/M_2=3$ /CUBIC STATES/LINEAR PARAMETERS/LINEAR PARAMETERS

FIGURE 4.10



(4,1,2,C,L,C): $N=4/M_1=1/M_2=2$ /CUBIC STATES/LINEAR PARAMETERS/CUBIC PARAMETERS

FIGURE 4.11

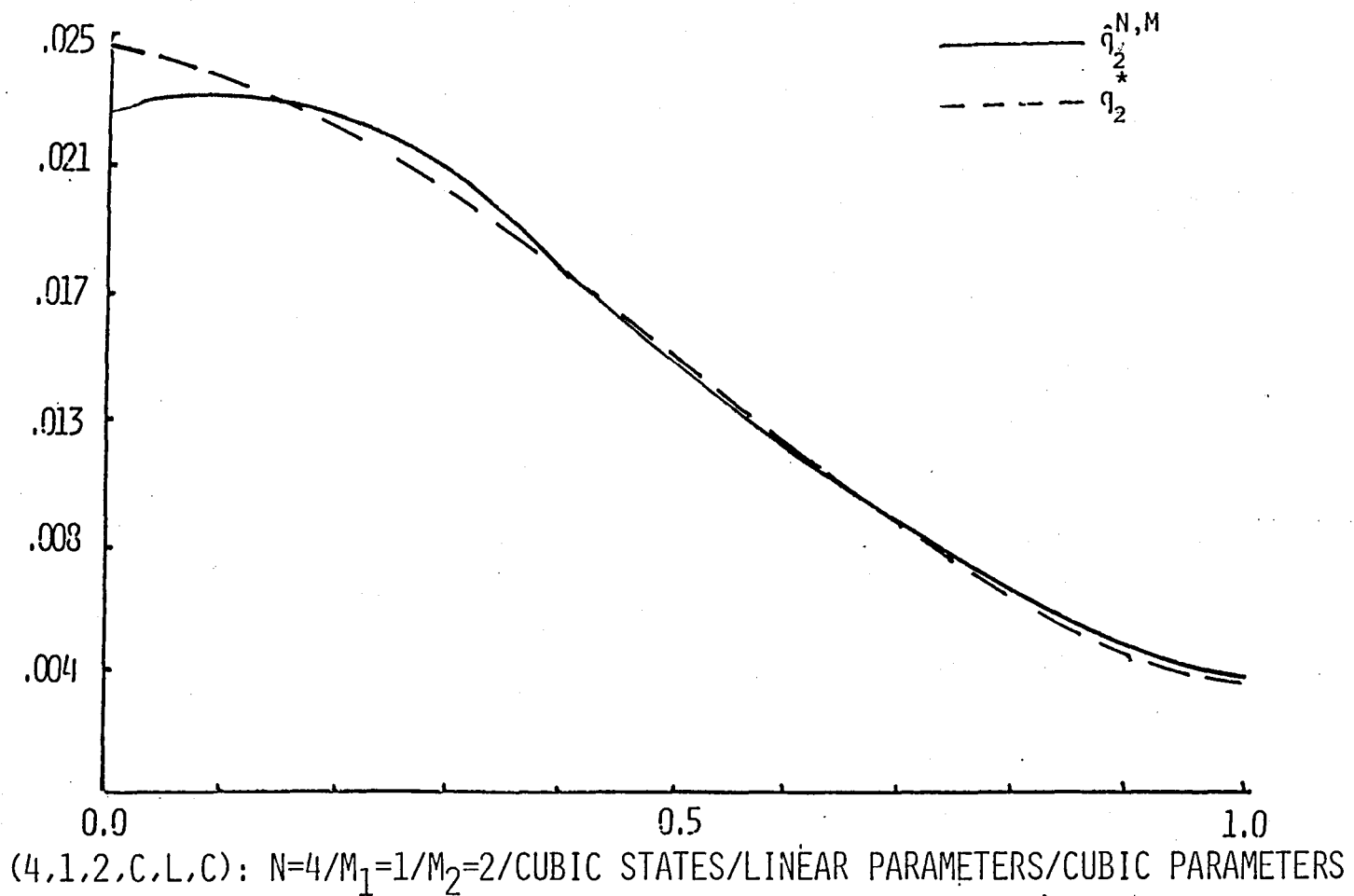


FIGURE 4.12

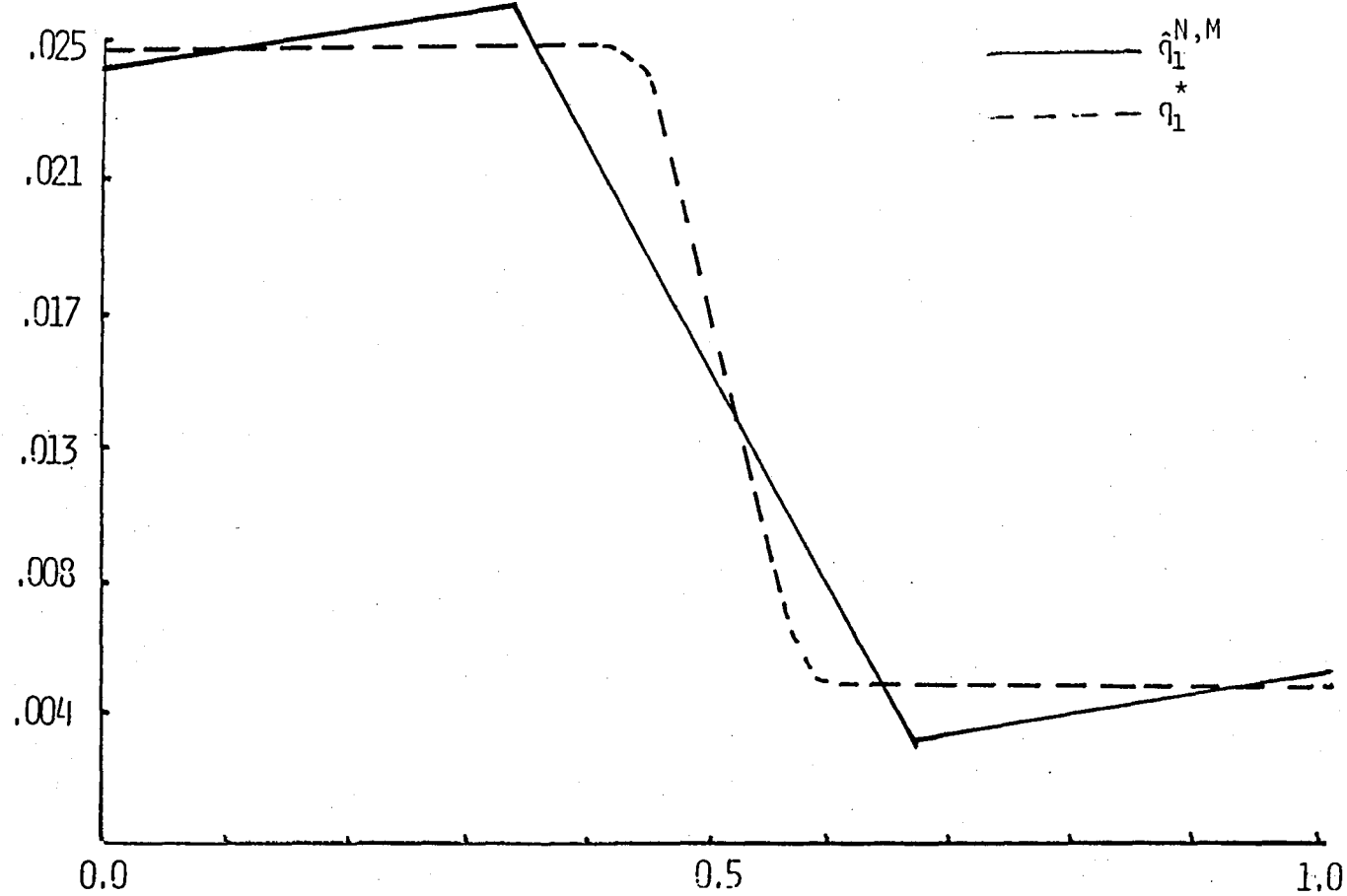
Example 5. We simultaneously estimate a variable stiffness coefficient,

$$q_1^*(x) = .1(1.5 - \tanh(20x - 10))$$

and a constant damping coefficient $q_2^* = .015$ for a cantilevered beam with tip body. We took $m=1.5$, $c=.1$, $J=.52$, $a_0=1$, $g(t) = 2e^{-t}$ and $h(t) = e^{-2t}$. Start up values were chosen as $q_1^0(x) = .15$, $0 \leq x \leq 1$, and $q_2^0 = .01$.

With a five cubic spline element state approximation ($N=4$), a two linear spline based discretization of the damping coefficient ($M_2=1$) and either a four linear spline ($M_1=3$) or a nine cubic spline ($M_1=6$) based discretization of the stiffness coefficient we obtained the results shown in Figures 4.13 - 4.16 with

$(N, M_1, M_2, S, P_1, P_2)$	$\hat{\phi}^{N,M}$	$E_1^{N,M}$	$E_2^{N,M}$
$(4, 3, 1, C, L, L)$	$.695 \times 10^{-7}$	$.174 \times 10^{-1}$	$.174 \times 10^{-3}$
$(4, 6, 1, C, C, L)$	$.195 \times 10^{-7}$	$.181 \times 10^{-1}$	$.550 \times 10^{-3}$



(4,3,1,C,L,L) : $N=4/M_1=3/M_2=1$ /CUBIC STATES/LINEAR PARAMETERS/LINEAR PARAMETERS

FIGURE 4.13

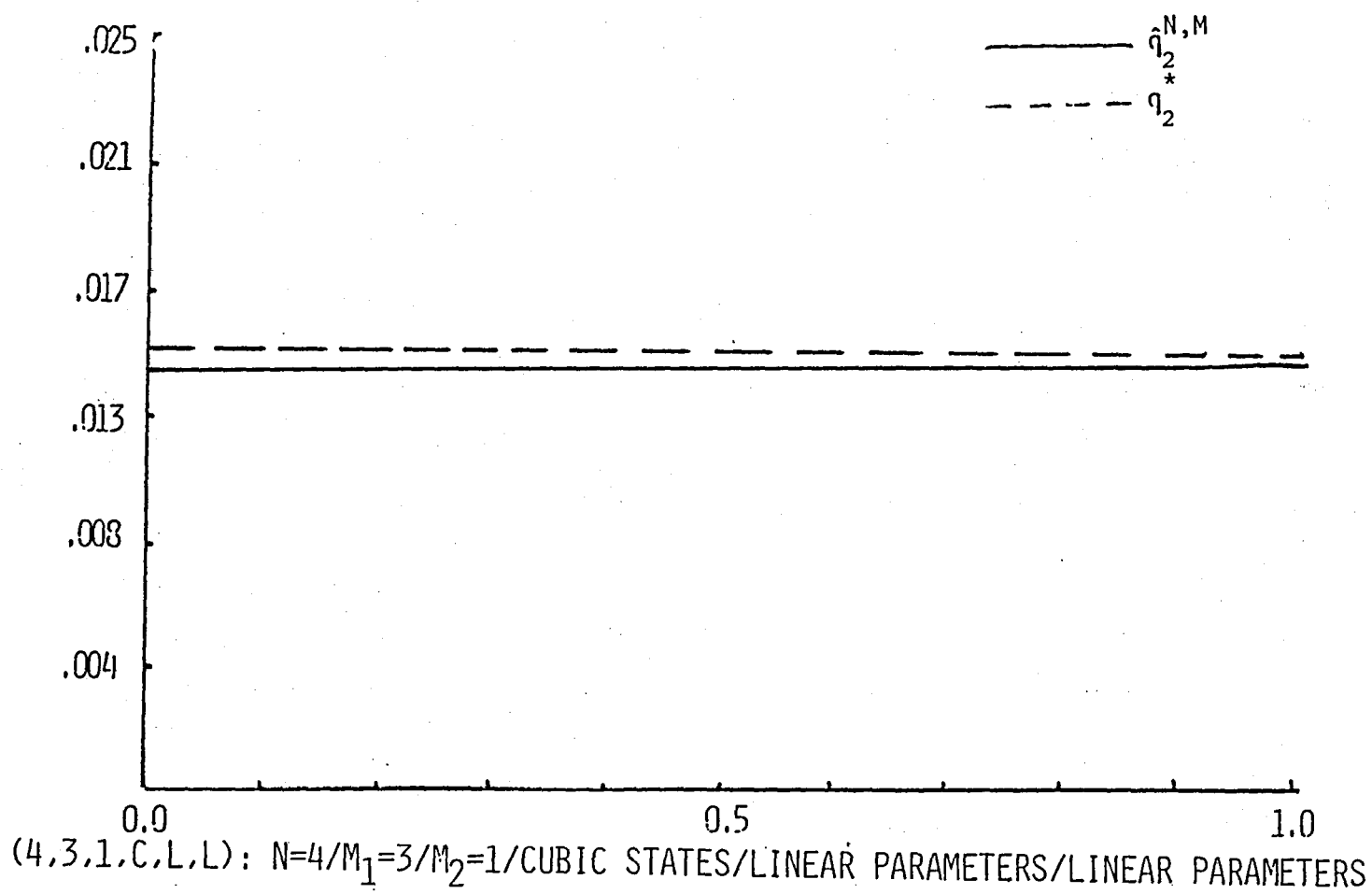


FIGURE 4.14

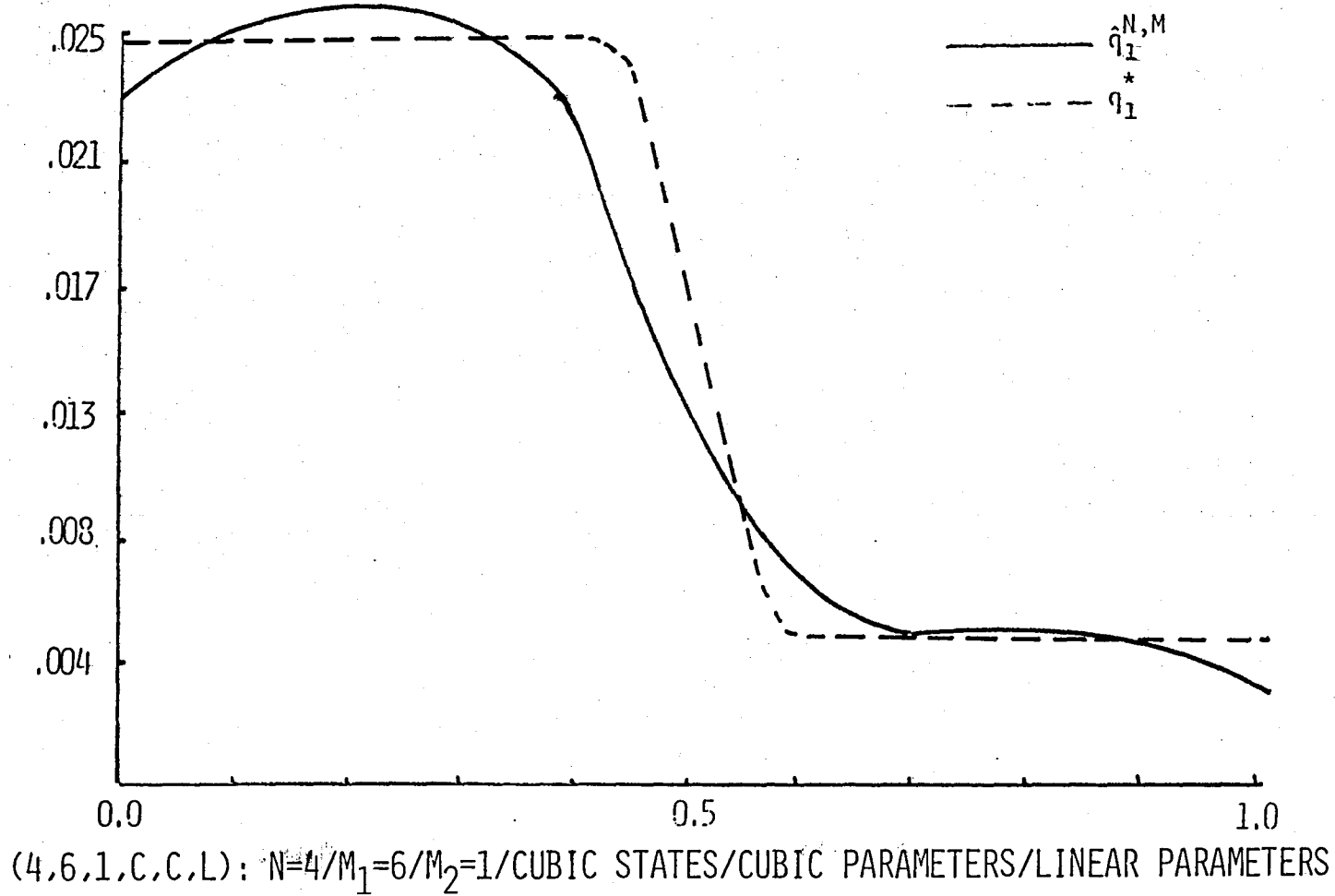


FIGURE 4.15

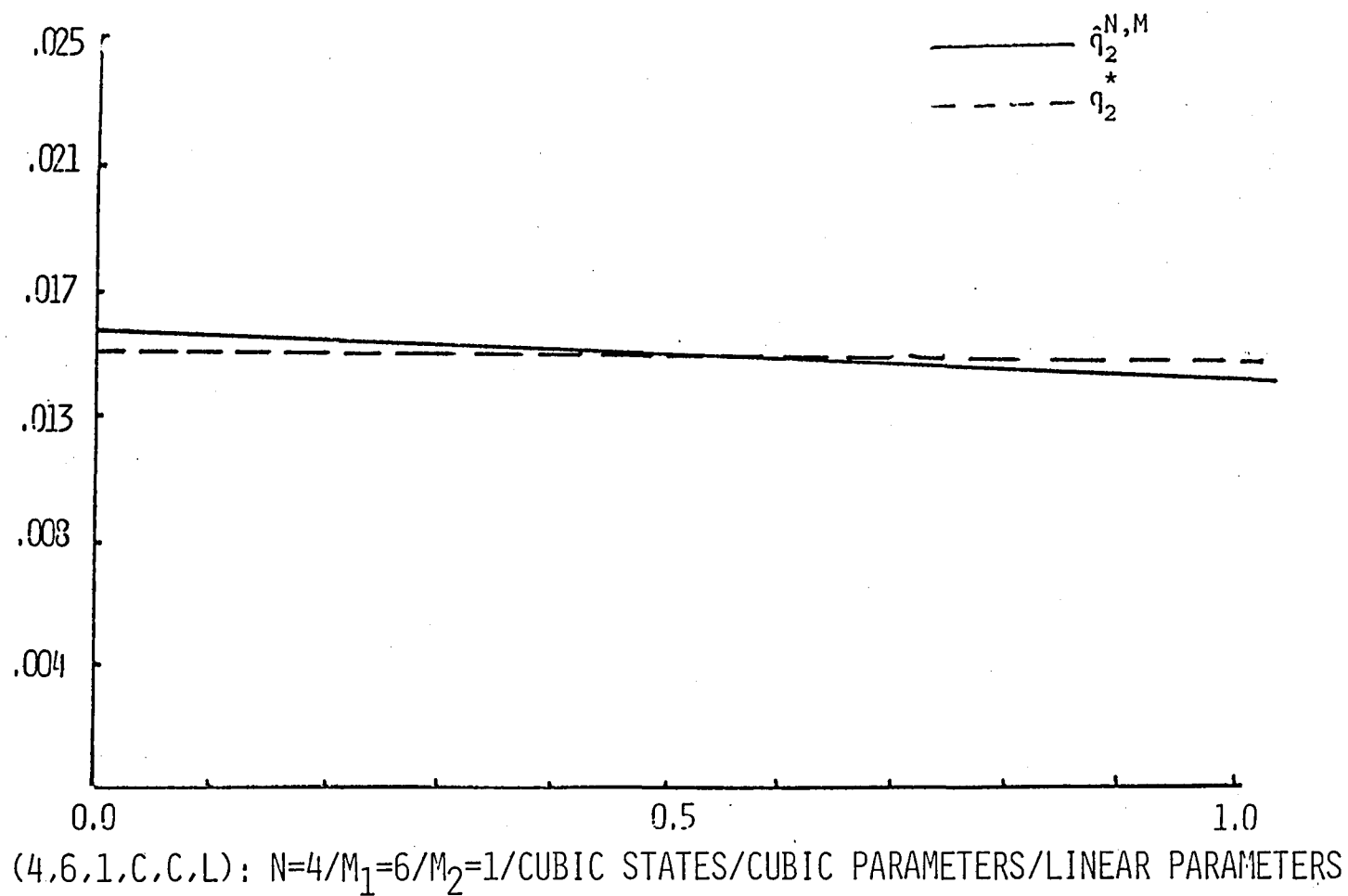


FIGURE 4.16

5. Concluding Remarks

We remark briefly on some of our findings as a result of the investigations described above as well as other related efforts. First, it is well-known that "inverse" problems such as we have considered here are often ill-posed, lacking a certain "stability" (i.e., lacking a continuous dependence of the estimated parameters $\hat{q}^{N,M}$ on the data $\{\tilde{u}_{ij}\}$). This can often lead to serious difficulties in computational efforts and it is sometimes helpful to use some type of regularization procedure in attempts to alleviate instabilities as well as speed up convergence. In much of our work we have taken an alternate approach, requiring that a compactness criterion be satisfied by the parameter set Q . Using arguments similar to some of those given in Section 2 above, one can argue that appropriate compactness assumptions on the parameter sets will guarantee a type of stability (e.g., see [1]). These compactness assumptions entail constraints that are sometimes "hard constraints" from a computational point of view, i.e., it is desirable to implement them in order to obtain a well-behaved computational procedure. As we noted above, in some of our "test" calculations with beam models, we have needed to impose the pointwise constraints of \tilde{Q} (which are weaker than the compactness constraints in this particular problem). As yet we have not tested the methods proposed in this paper with experimental data from beams (we are currently involved in projects to do this with beams of ordinary - e.g., steel- and composite materials). However, we have had considerable experience using similar methods with experimental data in other problems (climatology,

bioturbation, insect dispersal) involving second order partial differential equation models. To date we have found the algorithms we propose well-behaved, often only requiring the imposition of parameter constraints that are easily implemented and incorporated into the optimization schemes. We believe that this will also be the case in dealing with data from experiments with beams and other elastic structures.

Turning to a comment on the theoretical considerations of §2, we note that the presentations in [2], [3], [6], [25] employ a semigroup approximation approach (the Trotter-Kato theorem) that for the problems we consider here would require H^2 compactness of Q . The sesquilinear form arguments of [19] appear to require H^2 -weak compactness of Q as opposed to the \mathcal{L} compactness (in actuality, L^∞ compactness is sufficient and thus discontinuities can be allowed in the parameters if so desired) of this paper, [4], [5] and [10]. Given our comments above regarding stability of the associated computational algorithms, this relaxation could well be of more than just theoretical interest.

The methods described here did not, in general, perform as well when both a variable stiffness and damping coefficient were to be estimated simultaneously in our test example with beams. We are currently at work on a scheme that will deal more effectively with this more difficult class of problems.

We note that both the theoretical and computational ideas outlined in this paper are applicable to a wide class of problems including beams modeled with the Timoshenko theories [3] and two dimensional elastic structures [8]. For further discussion of the advantages/disadvantages of weak vs. strong formulations in parameter estimation problems, we refer to the reader to [1].

Finally, we remark that the numerical experiments outlined above (and others we have performed) are computationally intensive (even though for the examples of section 4 we always obtained convergence in 40 or less iterations in the optimization algorithm). Therefore, for conventional computational machines (e.g., sequential computers) use of these methods with experimental data could be expensive. However we believe that the approximation ideas and optimization schemes we are using offer great potential for use with emerging supercomputer technology (vector machines, attached array processors, parallel computers). In this regard, we are currently exploring the inherent parallelism and potential for vectorization of our algorithms and codes to develop fast, efficient software packages tailored to specific machine architectures. We are pursuing these efforts in the context of feedback control of distributed systems for elastic structures as well as for parameter estimation problems such as those considered above. Initial findings are quite encouraging and will be presented in a manuscript currently in preparation.

Acknowledgements

The authors would like to express appreciation to B. Hanks, J. Juang and E. Armstrong, NASA Langley Research Center, and K. Kunisch, Technische Universität Graz, for fruitful discussions in the course of this research.

References

- [1] H.T. Banks, On a variational approach to some parameter estimation problems, Proc. Int. Conf. on Control Theory for Distributed Parameter Systems and Applications, July 9-14, 1984, Vorau, Austria, Springer, to appear.
- [2] H.T. Banks and J.M. Crowley, Parameter estimation for distributed systems arising in elasticity, Proc. Symposium on Engineering Sciences and Mechanics, (National Cheng Kung University, December 28-31, 1981), pp. 158-177; LCDS Report #81-24, Brown University, November 1981.
- [3] H.T. Banks and J.M. Crowley, Parameter estimation in Timoshenko beam models, LCDS Report #82-14, Brown University, June 1982; J. Astronautical Sciences, 31, (1983), pp. 381-397.
- [4] H.T. Banks and J.M. Crowley, Parameter identification in continuum models, LCDS Report M-83-1, Brown University, March 1983; J. Astronautical Sciences, 33, (1985), pp. 85-94.
- [5] H.T. Banks and J.M. Crowley, Estimation of material parameters in elastic systems, LCDS Report #84-20, Brown University, June 1984.
- [6] H.T. Banks, J.M. Crowley, and K. Kunisch, Cubic spline approximation techniques for parameter estimation in distributed systems, IEEE Trans. Auto. Control, AC-28, (1983), pp. 773-786.
- [7] H.T. Banks and P.L. Daniel (Lamm), Estimation of variable coefficients in parabolic distributed systems, LCDS Report #82-22, Brown University, September 1982; IEEE Trans. Auto. Control, AC-30, (1985), pp. 386-398.
- [8] H.T. Banks, P.L. Daniel and E.S. Armstrong, A spline-based parameter and state estimation technique for static models of elastic surfaces, ICASE Report #83-25, NASA Langley Research Center, Hampton, VA, June 1983.
- [9] H.T. Banks and K.A. Murphy, Estimation of coefficients and boundary parameters in hyperbolic systems, LCDS Report #84-5, Brown University, February, 1984; SIAM J. on Control and Optimization, to appear.
- [10] H.T. Banks and I.G. Rosen, A Galerkin method for the estimation of parameters in hybrid systems governing the vibration of flexible beams with tip bodies, Rep. CSDL-R-1724, Charles Stark Draper Laboratory, Cambridge, MA, June 1984.
- [11] H.T. Banks and I.G. Rosen, Approximation techniques for estimation and feedback control for distributed models of large flexible structures, Proc. NASA/ACC Workshop on Identification and Control of Flexible Space Structures (June 4-6, 1984, San Diego); ICASE Report #84-26, NASA Langley Research Center, Hampton, VA, June, 1984.

- [12] G. Chavent, Identification of distributed parameter systems: About the output least squares method, its implementation, and identifiability, Proc. 5th IFAC Symp. on Identification and Systems Parameter Estimation, Pergamon Press, 1979, pp. 85-97.
- [13] C. C. Chen and C. T. Sun, Transient analysis of large frame structures by simple models, Proc. Symposium on Engineering Science and Mechanics, (National Cheng Kung Univ., Dec. 28-31, 1981), pp. 753-775.
- [14] G. Fairweather, Finite Element Galerkin Methods for Differential Equations, Marcel Dekker, New York, 1978.
- [15] R. Fletcher, Practical Methods of Optimization, John Wiley, New York, 1981.
- [16] P. Gill, W. Murray and M. Wright, Practical Optimization, Academic Press, New York, 1981.
- [17] A. C. Hindmarsh, GEAR: Ordinary differential equation system solver, Lawrence Livermore Laboratory, Report No. UCID-30001, Livermore, CA, 1972.
- [18] J. N. Juang and C. T. Sun, System identification of large flexible structures by using simple continuum models, J. Astronautical Sciences, 31, (1983), pp. 77-98.
- [19] K. Kunisch and E. Graif, Parameter estimation for the Euler-Bernoulli beam, Inst. für Math. Bericht 83-26, Techn. Universität Graz, December 1983; Mat. Aplicada e Computacional 4 (1985), pp. 95-124.
- [20] J. L. Lions, Optimal Control of Systems Governed by Partial Differential Equations, Springer, New York, 1971.
- [21] L. Nazareth, A conjugate directions algorithm without line searches, J. Opt. Theory Appl., 23, (1977), pp. 373-387.
- [22] A. K. Noor and C. M. Anderson, Analysis of beam-like lattice trusses, Comp. Meth. Appl. Mech. Engrg., 20, (1979), pp. 53-70.
- [23] D. W. Marquardt, An algorithm for least-squares estimation of nonlinear parameters, SIAM J., 11 (2), 1963.
- [24] P. M. Prenter, Spline and Variational Methods, Wiley-Interscience, New York, 1975.
- [25] I. G. Rosen, A numerical scheme for the identification of hybrid systems describing the vibration of flexible beams with tip bodies, Report CSDL-P-1893, Charles Stark Draper Laboratory, 1984; J. Math. Anal. Appl., to appear.

- [26] M. H. Schultz, Spline Analysis, Prentice-Hall, Englewood Cliffs, NJ, 1973.
- [27] C. T. Sun, B. J. Kim, and J. L. Bagdanoff, On the derivation of equivalent simple models for beam and plate-like structures in dynamic analysis, Proceedings AIAA Specialists Conference, Atlanta, Georgia, April 6-8, 1981, pp. 523-532.
- [28] J. Storch and S. Gates, Planar dynamics of a uniform beam with rigid-bodies affixed to the ends, Report CSDL-R-1619, Charles Stark Draper Laboratory, Cambridge, MA, 1983.
- [29] J. Storch and S. Gates, Transverse vibration and buckling of a cantilevered beam with tip body under axial acceleration, J. Sound and Vibration, 99, (1985), pp. 43-52.
- [30] J. Storch and S. Gates, Transverse vibration and buckling of a cantilevered beam with tip body under axial acceleration, Report CSDL-R-1675, Charles Stark Draper Laboratory, Cambridge, MA, 1983.

Appendix.

We outline here the computation of the gradients via a costate formulation. We recall (3.4)

$$\begin{aligned}\phi^{N,M}(\tilde{q}) &= J(u^N; q_1^M, q_2^M) \\ &= \sum_{i,j} |u^N(t_i, x_j; q^M) - \tilde{u}_{ij}|^2\end{aligned}$$

subject to (3.1) and (3.2)

$$\begin{aligned}u^N(t, x) &= \sum_{j=1}^{N+1} w_j^N(t) B_j^N(x) \\ q_i^M &= \sum_{j=0}^M q_{ij} b_j^M(x), \quad \tilde{q} = (q_{ij}),\end{aligned}$$

where $w^N = (w_1^N, \dots, w_{2N+2}^N)^T$ satisfies (3.3):

$$Q^{N \cdot N} w^N = K^N(q^M) w^N + f^N \quad (A.1)$$

$$Q^{N \cdot N} w^N(0) = w_0^N.$$

We note that w_0^N is independent of the parameters $q^M = (q_1^M, q_2^M)$ in the case considered here. We rewrite the cost criterion J as a functional over a continuum of t values by using Dirac functions δ . For each N we have

$$(A.2) \quad J = \sum_{i,j} \int_0^T \left| \sum_{k=1}^{N+1} w_k^N(t) B_k^N(x_j) - \tilde{u}_j(t) \right|^2 \delta(t-t_i) dt$$

where $\bar{u}_j(t) = \tilde{u}_{ij}$, $t_{i-1} < t \leq t_i$. For $q^M = (q_1^M, q_2^M)$ and R^{2N+2} vector functions w and p , we define the associated Lagrangian

$$(A.3) \quad \mathcal{L}(w, p, q^M) = \sum_{i,j} \int_0^T \left[\sum_{k=1}^{N+1} B_k^N(x_j) w_k(t) - \bar{u}_j(t) \right]^2 \delta(t-t_i) dt \\ + \int_0^T p^T(t) [Q^N w(t) - K^N(q^M) w(t) - f^N] dt$$

Note that for any vector function p we have, for $w = w^N$ the solution of (A.1),

$$(A.4) \quad \phi^{N,M}(\tilde{q}) = \mathcal{L}(w^N(q^M), p, q^M),$$

so that

$$(A.5) \quad \frac{\partial \phi^{N,M}}{\partial q_{ij}} = d\mathcal{L}[w^N, p, q^M; \frac{\partial w^N}{\partial q_{ij}}] + \frac{\partial \mathcal{L}}{\partial q_{ij}}(w^N, p, q^M)$$

for $i = 1, 2, j = 0, 1, \dots, M$, where $d\mathcal{L}$ is the differential of \mathcal{L} with respect to the vector function w . Thus the expression for the desired gradients can be greatly simplified if p is chosen so that $d\mathcal{L}[w^N, p, q^M; v] = 0$ for any variation function v (which we note must satisfy $v(0) = 0$ since w_0^N is independent of q^M). To do this, we must compute the differential $d\mathcal{L}$. We have

$$d\mathcal{L}[w^N, p, q^M; v] =$$

$$\int_0^T \left\{ 2 \sum_{i,j} \left[\sum_k B_k^N(x_j) w_k^N(t) - \bar{u}_j(t) \right] \delta(t-t_i) \sum_{\ell} B_{\ell}^N(x_j) v_{\ell}(t) \right.$$

$$\begin{aligned}
 & + p^T(t) [Q^N \dot{v}(t) - K^N(q^M) v(t)] \Big\} dt \\
 & = \int_0^T \left\{ \sum_i \gamma^N(t)^T \delta(t-t_i) v(t) + p^T(t) [Q^N \dot{v}(t) - K^N(q^M) v(t)] \right\} dt
 \end{aligned}$$

where γ^N is the R^{2N+2} vector function given by

$$(A.6) \quad \gamma_\ell^N(t) = \begin{cases} 2 \sum_j [\sum_k B_k^N(x_j) w_k^N(t) - \bar{u}_j(t)] B_\ell^N(x_j), & \ell = 1, 2, \dots, N+1, \\ 0 & \ell = N+2, \dots, 2N+2. \end{cases}$$

Integrating by parts on the obvious term in the expression for $d\mathcal{L}$ and using $v(0) = 0$, we find

$$\begin{aligned}
 d\mathcal{L} &= \int_0^T \left\{ -\dot{p}^T(t) Q^N - p^T(t) K^N(q^M) + \sum_i \gamma^N(t)^T \delta(t-t_i) \right\} v(t) dt \\
 &+ p^T(T) Q^N v(T).
 \end{aligned}$$

Thus $d\mathcal{L} = 0$ for all v if we choose p a solution of

$$\dot{p}^T(t) Q^N + p^T(t) K^N(q^M) - \sum_i \gamma^N(t)^T \delta(t-t_i) = 0$$

$$p(T) = 0,$$

or since Q^N is a $2N+2$ square symmetric matrix,

$$(A.7) \quad Q^N \dot{p}(t) = -(K^N(q^M))^T p(t) + \sum_i \gamma^N(t) \delta(t-t_i)$$

$$p(T) = 0.$$

Returning to (A.5) we thus find

$$(A.8) \quad \frac{\partial \phi^{N,M}}{\partial q_{ij}} = \frac{\partial \mathcal{L}}{\partial q_{ij}}(w^N, p, q^M) = \int_0^T -p^T(t) \left[\frac{\partial K^N(q^M)}{\partial q_{ij}} \right] w^N(t) dt,$$

$$i = 1, 2, j = 0, 1, \dots, M.$$

Recalling the definition of $K^N(q)$ - see (3.3) - and the representation (3.2), we find

$$(A.9) \quad \frac{\partial \phi^{N,M}}{\partial q_{ij}}(\tilde{q}) = - \int_0^T p^T(t) \mathcal{K}_{ij} w^N(t) dt$$

for $i = 1, 2, j = 0, 1, \dots, M$, where the $2N+2$ square matrices \mathcal{K}_{ij} are given by

$$(A.10) \quad \mathcal{K}_{1j} = \begin{bmatrix} 0 & 0 \\ \mathcal{D}_j & 0 \end{bmatrix},$$

$$(A.11) \quad \mathcal{K}_{2j} = \begin{bmatrix} 0 & 0 \\ 0 & \mathcal{D}_j \end{bmatrix}, \quad j = 0, 1, \dots, M$$

with \mathcal{D}_j the $N+1$ square matrix with elements

$$(A.12) \quad [\mathcal{D}_j]_{i,k} = \int_0^1 b_j^{M,2} b_i^{N,2} b_k^{N,2} dx.$$

The costate equations (A.7) can be transformed for convenience. Defining

$$\begin{aligned} P(t) &= p(t) - [Q^N]^{-1} \int_0^t \sum_i \gamma^N(s) \delta(s-t_i) ds \\ &= p(t) - [Q^N]^{-1} \sum_{t_i \leq t} \gamma^N(t_i), \end{aligned}$$

we may compute the solution P of

$$\begin{aligned} (A.13) \quad Q^N \dot{P}(t) &= -K^N(q^M)^T \left\{ P(t) + [Q^N]^{-1} \sum_{t_i \leq t} \gamma^N(t_i) \right\} \\ Q^N P(T) &= - \sum_i \gamma^N(t_i). \end{aligned}$$

This is then used to obtain p by

$$(A.14) \quad p(t) = P(t) + [Q^N]^{-1} \sum_{t_i \leq t} \gamma^N(t_i)$$

which in turn is used in (A.9) to compute the desired gradients.

Standard Bibliographic Page

1. Report No. NASA CR-178135 ICASE Report No. 84-66		2. Government Accession No.		3. Recipient's Catalog No.	
4. Title and Subtitle METHODS FOR THE IDENTIFICATION OF MATERIAL PARAMETERS IN DISTRIBUTED MODELS FOR FLEXIBLE STRUCTURES				5. Report Date May 1986	
				6. Performing Organization Code	
7. Author(s) H. T. Banks, J. M. Crowley, I. G. Rosen				8. Performing Organization Report No. 84-66	
9. Performing Organization Name and Address Institute for Computer Applications in Science and Engineering Mail Stop 132C, NASA Langley Research Center Hampton, VA 23665-5225				10. Work Unit No.	
				11. Contract or Grant No. NAS1-16394, NAS1-17130	
12. Sponsoring Agency Name and Address National Aeronautics and Space Administration Washington, D.C. 20546				13. Type of Report and Period Covered Contractor Report	
				14. Sponsoring Agency Code 505-31-83-01	
15. Supplementary Notes Langley Technical Monitor: Submitted to Matematica Aplicada e J. C. South Computacional Final Report					
16. Abstract In this paper we present theoretical and numerical results for inverse problems involving estimation of spatially varying parameters such as stiffness and damping in distributed models for elastic structures such as Euler-Bernoulli beams. An outline of algorithms we have used and a summary of our computational experiences are presented.					
17. Key Words (Suggested by Authors(s)) parameter estimation, computational methods, Euler-Bernoulli beams				18. Distribution Statement 64 - Numerical Analysis 66 - Systems Analysis Unclassified - unlimited	
19. Security Classif.(of this report) Unclassified		20. Security Classif.(of this page) Unclassified		21. No. of Pages 60	
				22. Price A04	

End of Document